Validation of Satellite Ozone Measurements Over Nairobi Using MAX-DOAS 2003-2004

A fourth year project at the
Department of Physics, University of Nairobi.

By
Jonas Lähnemann
I20 / 3148 / 2004

Supervisor: Dr. Angeyo Kalambuka

July 2005

In memory of my teacher
Prof. Bodo Hamprecht,
a great and inspiring lecturer and
longtime supporter of the Berlin-Nairobi Exchange,
who died in a bicycle accident
during the time of my stay in Nairobi.

Abstract

This work presents a study of total column ozone from ground-based DOAS measurements in Nairobi and overpass data from satellite instruments (TOMS, GOME and SCIAMACHY) for the years 2003 and 2004. The long-term record of TOMS shows no depletion of total column ozone above this tropical location with an average concentration of 260 DU, besides annual and biennial oscillations between 40-60 DU. From the comparison of the DOAS record with the data from TOMS, GOME and SCIAMACHY, as well as the ozonesondes, a very good agreement in trend was concluded for all instruments, as the root-mean-square values of the deviations from DOAS are all below 3.5% and the mean deviations are even less ($< 1.5\%$). Correlation between the different data sets is also very good for most of the time observed, with a deviation $< 5\%$. It can be concluded that the Bremian algorithm for the analysis of SCIAMACHY data yields good results for total column ozone. After comparing the 2003-2004 period, where the lowest ozone values were recorded for the first and last months, with the long-term TOMS record, it was infered that this work covers exactly one cycle of the Quasi-Biennial Oscillations (QBO). A special feature of the MAX-DOAS instrument are off-axis viewing directions close to the horizon, showing stronger signals of tropospheric absorbers than zenith-sky observations. Ozone slant columns of different viewing directions were, however, found to be so close to each other that no information about tropospheric concentrations can be retrieved for ozone. For the verification of satellite measurements and to obtain a long-term record of different trace gases for a tropical location, every effort should be made not only to maintain operation of the MAX-DOAS instrument in Nairobi, but also to continuously evaluate the retrieved data.

Contents

1 Introduction

Ozone (O_3) is an important but toxic molecular species in the troposhere. In the stratosphere ozone absorbs most of the ultra-violet (UV) radiation, preventing this potentially harmful radiation from reaching the earth's surface and accounting for the temperature increase in this atmospheric layer and thus for the stability of the atmosphere. Ozone is formed and destroyed in complex systems of atmospheric chemical reactions, catalyzed by various other trace gases.

With increased industrialization, rising emissions of pollutant gases have led to a rise in ozone levels close to the ground. This can be part of the so-called smog. Pollution is also responsible for a decline in the stratospheric ozone concentration, especially in the antarctic region, there known as ozone hole. Currently these are still very pressing environmental issues.

Different techniques have been developed and utilized to monitor the Ozone concentrations in the atmosphere over the years. Among them are passive spectroscopic systems using sunlight; these have the advantage that they can yield total columns of atmospheric trace gases and to a certain extent information about the vertical distribution of these trace gases. One of the passive spectroscopic methods is the Differential Optical Absorption Spectroscopy (DOAS) [Perner and Platt, 1979]. In the DOAS technique the absorption profiles in the observed sun-spectra are used to calculate the concentrations of the absorbants. Besides ground based spectroscopical systems, giving information on the diurnal variation of the observed species, these methods can be deployed in aircraft and on satellites, the latter allowing for global coverage. Other techniques for monitoring ozone include chemical *in situ* measurements and LIDAR.

Spectroscopic measurements of atmospheric ozone have been made since the 1930s (e.g. Dobson Spectrometers [Dobson, 1968]). In the 70s the DOAS method was developed. A current development is the implementation of MAX-DOAS (Multi-Axis DOAS) in which measurements at different zenith angles with varying lightpaths in the troposphere are used to extract limited information on the vertical distribution of ozone [Wittrock et al., 2004].

Since August 2002 the University of Bremen has been operating a MAX-DOAS system at the UNEP campus in Gigiri, Nairobi. This instrument can be used to measure the columns of atmospheric trace gases, such as O_3, NO_x, BrO or OClO. It is part of a Bremen based network with stations in different latitudes offering possibilities for the validation of satellite based measurements of trace gases. Such measurements are for example carried out with the EP/TOMS, GOME or SCIAMACHY instruments. The Nairobi DOAS station, in continuously monitoring the atmosphere, also fills a gap of measurements in a tropical, especially urban, location. Though its main focus are total

columns of trace gases, with the off-axis measurements being directed towards the city center of Nairobi, the measurements also yield some information about the smog situation in Nairobi [Wittrock et al., 2004; Adupko, 2002].

To retrieve a more detailed profile of the vertical distribution of ozone, balloon launches are being carried out in many places in the world. As measurements for the southern hemisphere, especially for the tropical regions, had been lacking, NASA's Goddard Space Flight Center (GSFC) introduced the Southern Hemisphere Additional Ozonesondes (SHADOZ) program in 1998. Nairobi, with weekly sonde launches, is one of the stations supported. [Thompson et al., 2004]

This work is aimed at comparing data from the ground-based MAX-DOAS station in Nairobi and satellite instruments (TOMS, GOME and SCIAMACHY) for SCIAMACHY validation purposes, as well as looking at the relating SHADOZ sonde data. The time period considered are the years 2003 and 2004. The focus will be on total column ozone, as this is easily retrieved from the remote sensing instruments and offers a way to compare the different data sets. With the help of the TOMS measurements, which have been going on since 1979, the time under investigation can be placed in a long-term perspective. Total columns of ozone mainly yield information about stratospheric concentrations, as 90% of atmospheric ozone reside here. With more complex algorithms it is possible to calculate tropospheric columns from the ground-based and satellite instruments: It therefore shall be determined if the multi-axis setup of the Nairobi DOAS allows the separation of stratospheric and tropospheric absorption by ozone. The sonde data, on the other hand, readily provides vertical profile information. The DOAS is also envisaged to yield information on the diurnal variation of ozone columns.

The work is structured in the following way: An overview of the ozone chemistry in the earth's atmosphere is presented in the second chapter. Besides summarizing the processes governing tropospheric and stratospheric ozone concentrations and their impact, issues special to the tropical region are considered. Then an introduction to the experimental setup of the Multi-Axis DOAS (MAX-DOAS) instrument and to the DOAS technique is given in the third chapter, followed by information on different satellite based systems (TOMS, GOME and SCIAMACHY) and ozonesonde soundings. The fourth chapter is dedicated to the data analysis and comparison. Finally the results are summarized in the fifth chapter.

2 Atmospheric Chemistry

The atmosphere is the gaseous area surrounding our planet. Up to about 80 km it consists of a relatively stable mixture of gases, the major components being nitrogen (78%), oxygen (21%) and argon (0.93%); refer to table 2.1 for further details. Also present are water vapor and relatively small quantities of different trace gases, however, in a far more variable concentration and distribution. It is these trace gases that mainly govern the atmospheric chemistry and temperature distribution processes in which ozone plays a key role as reactant.

2.1 Tropospheric Ozone

The troposphere is the layer closest to the earth's surface. Its height is variable: Extending up to about 20 km around the equator and up to around 8 km in polar regions; this, however, depends on the season (highest in the summer and lowest in the winter).

Trace gas concentrations in this stratum are determined by different sources and sinks, the interaction with the Biosphere and Hydrosphere playing a key role. They can be released by natural processes (biological emissions from organisms, biomass burning, volcanoes) or as result of human activity, characterized as pollution (burning of fossil fuels, agriculture, etc.); and they can also be produced through, often photochemical, reactions from other gases.
Their elimination is also partly through chemical reactions, as well as wet removal (dissolved in rain), dry deposition (on the soil and oceans) and assimilation into organisms. The Stratospheric-Tropospheric Exchange (STE) of gases is both a source and a sink for tropospheric species. The transport and mixture of these gases within the troposphere is determined by weather phenomena.

Although its concentration in the troposphere is rather small (approximately 10% of the atmospheric ozone resides here, see figure 2.1), ozone plays a major role in the

Table 2.1: *Composition of dry unpolluted air by volume. [Brimblecombe, 1996]*

Nitrogen	78.084%	Methane	1.6 ppm
Oxygen	20.946%	Krypton	1.14 ppm
Argon	0.934%	Hydrogen	0.5 ppm
Carbon dioxide	360 ppm (variable)	Nitrous Oxide	0.3 ppm
Neon	18.18 ppm	Xenon	0.087 ppm
Helium	5.24 ppm		

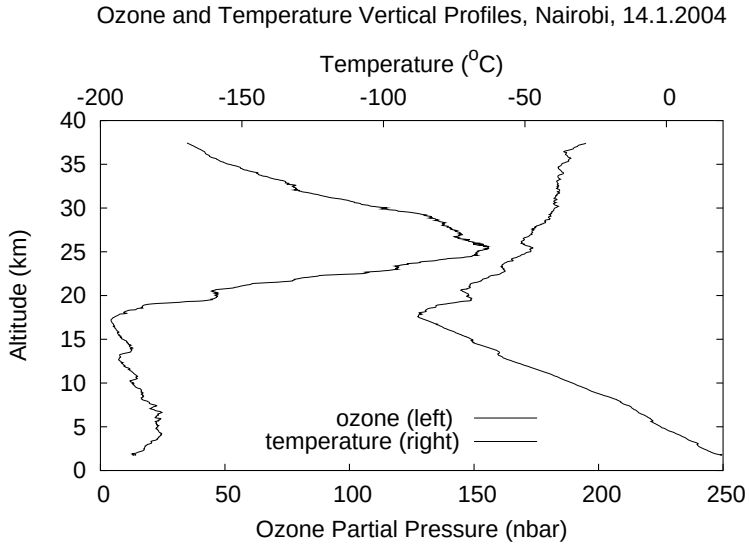

Figure 2.1: *Vertical profile of ozone in the atmosphere [SHADOZ Ozonesonde Data]. The left curve shows the ozone profile from ground level to about 37 km, while the right curve shows the temperature profile. Obvious is the rise in temperature through absorption of UV light in the stratospheric ozone layer.*

tropospheric chemistry. While elevated concentrations at ground level are toxic for humans and plants (see section 2.1.4), ozone, on the other hand, is important as reactant and so in reducing the concentrations of other pollutants. In the higher troposphere it serves as a greenhouse gas contributing to the greenhouse effect (section 2.1.2).

2.1.1 Sources and Role of Tropospheric Ozone

Tropospheric ozone has two sources: (1) Stratospheric-Tropospheric Exchange, where ozone is formed in the stratosphere through photolysis from O_2 (see section 2.2) and is transported into the troposphere. Photolysis of O_2 does not take place in the troposphere as the necessary radiation of short wavelength (< 242 nm) is completely absorbed in the stratosphere.
(2) Reaction of O_2 with O, where atomic oxygen results from photolysis of NO_2:

$$NO_2 + h\nu \rightarrow NO + O \tag{2.1}$$

$$O + O_2 + M \rightarrow O_3 + M \tag{2.2}$$

with the absorbed light being of wavelength $\lambda \leq 420$ nm and M representing another molecule carrying away excess energy.
O_3 can react back with NO to return NO_2

$$O_3 + NO \rightarrow NO_2 + O_2 \tag{2.3}$$

However, as ozone is highly reactive it also interacts with many other species. To achieve the often higher levels of ozone than accounted for by the above reactions,

other processes involving NO_x[1], carbon monoxide (CO), hydrocarbons (HCs) and non-methane hydrocarbons (NMHCs) in combination with hydrogen oxides (OH) and photon energy from sunlight ($h\nu$) are also of importance; either they lead to reactions (2.1) and (2.2) or they offer an alternative to the oxidation of NO through reaction (2.3).

Ozone plays a central role in the chemistry of the troposphere. It initiates the oxidation of other molecules through its responsibility in forming reactive oxidants. The major oxidant behind many atmospheric reactions is the hydroxyl radical OH, formed from O_3 during daytime through photolysis[2]:

$$O_3 + h\nu \rightarrow O_2 + O^* \quad (2.4)$$

$$O^* + H_2O \rightarrow 2\ OH \quad (2.5)$$

The so produced OH is in turn responsible for oxidizing CO and volatile organic compounds (VOCs, i.e. HCs and NMHCs, among others) some of which again lead to ozone production or reduction. OH is also involved in chains of reactions leading again to reaction (2.1). A broader discussion, putting these reactions into the context of the more complex processes governing ozone concentrations may be found elsewhere [Warneck, 1988; Brimblecombe, 1996].

2.1.2 The Greenhouse Effect

The earth maintains a stable average temperature and therefore a stable climate through a balance of energy lost to space with the energy received by the earth from the sun (refer to figure 2.2). Short wavelength radiation (UV and visible) reaches the earth from the sun (a black body of approximately 6000°K). This radiation is either absorbed or reflected by the atmosphere and clouds or at the earth's surface. On the other hand, the earth itself is a radiating body, though this is radiation of a longer wavelength (infrared), as the earth's temperature is much cooler.

The trace gases in the atmosphere absorb light in certain wavelength regions, while they let other wavelengths pass through. Generally visible light passes through unimpeded so that we can see the sun. Among the atmospheric trace gases are greenhouse gases, such as CO_2, CH_4, NO_2 and O_3, which absorb electromagnetic radiation in the infrared region emitted by the earth. This prevents some of the radiation from escaping to space and heats the atmosphere, causing the earth to store more energy close to its surface – a prerequisite for life on earth by allowing water to exist in a liquid form.

A question still discussed controversially in the scientific community is how far a rise in the concentrations of greenhouse gases from anthropogenic sources is a cause for the global warming observed during the last century. The Intergovernmental Panel on Climate Change acknowledged the role of anthropogenic sources [IPCC, 2001]. A scientific

[1] NO_x = NO and NO_2

[2] O^* stands for an exited oxygen atom

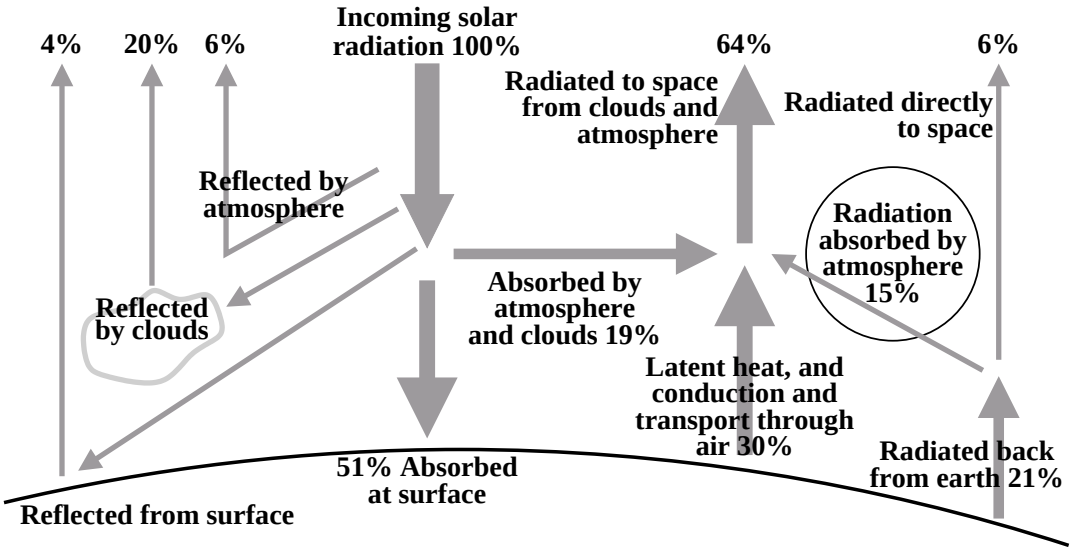

Figure 2.2: *The earth's energy balance. The graph shows absorption and reflection of solar radiation and the earth's radiation of long wavelengths. The part played by the greenhouse effect is highlighted with a circle.*

consensus on this was also concluded by Oreskes [2004] in a survey of peer-reviewed scientific abstracts.

2.1.3 Photochemical Smog

The rise of tropospheric ozone concentrations, especially in urban and industrial regions, but probably also on a global scale, during the past century or so is a direct result of the increased emissions of its precursors from anthropogenic sources (mainly fossil fuel burning in traffic and energy production). The extreme of this rise being the occurrence of photochemical smog in urban centers.

Smog is a mixture of gases forming a haze over cities during periods where emissions of primary pollutants (SO_2, NO_x and CO_x) are not sufficiently ventilated in the absence of wind, while strong solar radiation leads to the photochemical formation of secondary pollutants (most prominently O_3). Generally the stagnation of the air masses is a result of a temperature inversion above the ground. Topographical factors, like surrounding mountains, can also play a role.

This form of smog was first characterized above Los Angeles in the 1950s, but due to the rise in traffic and other urban sources is now common in most tropical and subtropical cities. In the mid latitudes it can appear during summer months.

The diurnal evolution of some key chemical players in the urban atmosphere is illus-

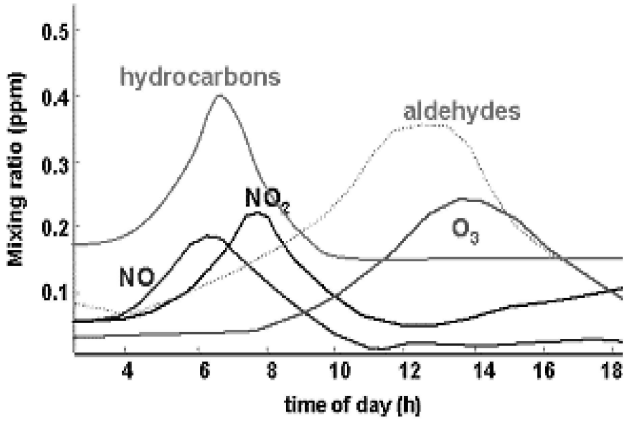

Figure 2.3: *Diurnal evolution of key chemical players (NO_x, O_3, hydrocarbons and aldehydes) in the urban atmosphere. [Akeem, 2003]*

trated in figure 2.3. The emissions of NO_x and VOCs (like hydrocarbons) increase with the morning rush hour. When later in the morning traffic reduces, NO and VOCs begin to react and form NO_2 resulting in a rise of its concentration.
With intensifying sunlight around noon and in the early afternoon hours NO_2 is broken down and the so released oxygen can form the increasing concentrations of ozone according to reactions (2.1) and (2.2). Simultaneously through a reaction of NO_2 with the VOCs toxic chemicals such as Peroxylacetyl Nitrate (PAN) are produced.
When the sun goes down in the evening, O_3 production stops and its concentration is reduced by various reactions. A factor in this being again the NO_x emissions from the evening rush hour with their double role as source and sink of ozone (see reaction (2.3)). Despite this nighttime reduction the ozone level can increase from day to day during a smog episode. Highest ozone levels, however, are actually found in the surroundings of cities, where it is transported but then not broken down by NO_x from traffic emissions. The elevated ozone levels have negative effects on all living organisms.

2.1.4 Effects of Ground Level Ozone

Exposure to higher levels of ozone and synergisms with other pollutants can lead to respiratory effects, including coughs, throat dryness thoracic pain and increased mucous production in humans. Even healthy individuals are at risk, but an increased number of asthma patients might also be linked to increased tropospheric ozone. The 1987 WHO recommendation gives exposure to 150-200 μg m^{-3} (0.076-0.1ppm) of ozone over one hour or 100-120 μg m^{-3} (0.05-0.06 ppm) for the 8h range as limits for air quality standards.

Plants are even more sensitive to air pollutants. Ozone, as primary agent of the photochemical Los Angeles smog, was linked to damage found among leafy vegetables,

like lettuce, prompting research as early as the 1950s. Ozone was also recognized as a reason for the decline of lichen species in the forests near Los Angeles. Brief periods of very high concentrations, but also long periods of slightly raised ozone levels during the summer months can lead to a reduction in crop yields due to impairment of photosynthesis.

Additionally ozone, as photoxidant, can degrade synthetic materials like nylon and rubber. Therefore for some exposed uses, like in tires, alterations to the materials had to be made, to protect them better against damage by ozone. [Brimblecombe, 1996]

2.2 Stratospheric Ozone

The stratosphere is extending up to about 50 km from the tropopause and ozone is the most important trace gas in this layer, with about 90% of atmospheric ozone being located here (mainly between 15 and about 40 km in what is called the ozone layer). In this atmospheric region the temperature is rising again (see figure 2.1), due to the absorption of light by ozone, especially in the UV region, which in turn protects life on earth from this harmful radiation. The role of ozone in this abrupt cutoff of the solar spectrum at 300 nm was already proposed by Hartley in 1880.

This atmospheric layer is characterized by its stability, as in the absence of weather phenomena (wind, precipitation) comparatively little vertical motion and mixing takes place. For the same reason, materials that enter the stratosphere, be it from volcanic eruptions, anthropogenic chemicals carried across the tropopause or emissions from aircraft, can remain there for long periods of time as they are not deposited or removed by rain. This means the only sources for trace gases in the stratosphere are transport from the troposphere, a limited amount of direct emissions, and photochemical reactions. The only sinks are transport to other atmospheric layers and reactions (which actually are only a temporary sink).

2.2.1 Sources and Sinks of Stratospheric Ozone

The Chapman Cycle [Chapman, 1930], proposed as theory explaining stratospheric ozone concentrations, presumes that production and dissociation of O_3 in the stratosphere is only to and from O_2.

The formation of ozone is through the dissociation of O_2 by solar UV radiation (with $\lambda < 242$ nm), where the atomic oxygen then reacts to molecular oxygen to form ozone (M represents either N_2 or O_2):

$$O_2 + h\nu \rightarrow 2\ O \tag{2.6}$$

$$O + O_2 + M \rightarrow O_3 + M \tag{2.7}$$

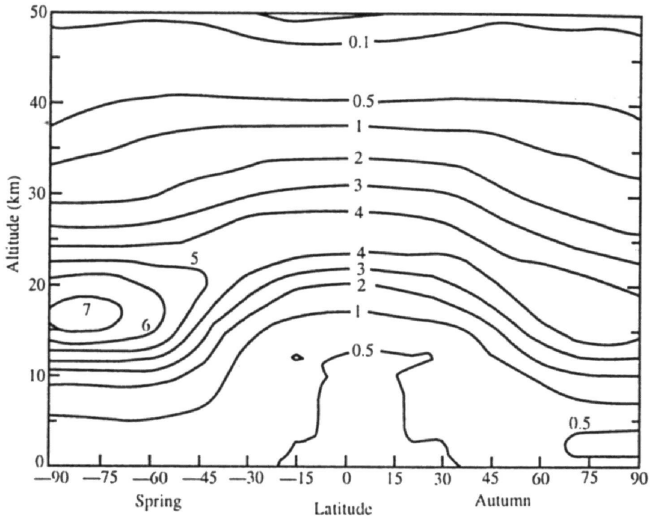

Figure 2.4: *The natural ozone layer: Vertical and latitudinal distribution of the ozone number density (1012 molecules cm^{-3}) at the equinox, based on measurements taken in the 1960s. [Adupko, 2002]*

Chapman also proposed the photodissociation of O_3 and following production of O_2 as a sink for ozone:

$$O_3 + h\nu \rightarrow O_2 + O \tag{2.8}$$
$$O + O_3 + M \rightarrow 2\ O_2 \tag{2.9}$$

These reactions, however, cannot predict the right concentrations of ozone. Instead, several other catalytic chemical cycles are involved in the removal of stratospheric ozone. They are basically of the form

$$X + O_3 \rightarrow XO + O_2 \tag{2.10}$$
$$XO + O \rightarrow X + O_2 \tag{2.11}$$

Here X represents the catalyst, while XO is the intermediate product. Among the most common catalysts are NO, ClO, BrO, OH and H. These species only catalyze the destruction of ozone and a single molecule can be responsible for the destruction of many molecules of O_3. While some of them are part of the natural balance, even minor constituents of the upper atmosphere resulting from human activity can have major effects on the ozone concentrations in this strata.

As the stratosphere is "dry", the OH radical does not play such a central role as in the troposphere. Ozone, on the other hand, is again a key player in many of the chemical processes present.

2.2.2 Perturbations of the Natural Balance

The natural, but also most anthropogenic sources, of the catalysts involved in breaking up stratospheric O_3 are located in the troposphere, with the substances being slowly transported up through the tropopause. Only emissions from volcanoes and high flying aircraft are directly inserted into the stratosphere. Human-caused disturbance of the ozone layer originates mostly from emissions in the troposphere and there mainly in the planetary boundary layer.

With the industrialization, sources of some of the reactants involved in the catalytic destruction of ozone have increased significantly. Of special concern are stable compounds of Chlorine (Cl). This was first documented for chlorofluorocarbons (CFCs), usable for example as nontoxic, nonflammable refrigerant and as propellant in aerosol cans. As they have a long lifetime in the troposphere – not being soluble in water, not easily oxidized by OH and not photoactive at wavelengths above 300 nm – they are eventually mixed and can reach the stratosphere. There the short wavelength UV light can break these stable molecules up into their more reactive forms Cl and ClO, ready to go through reactions (2.10) and (2.11). After their major influence in the destruction of the ozone layer and causing of the ozone hole was detected, CFCs were rather effectively banned and replaced in the 1990s. Due to their long lifetime it will, however, take another 50 years until their effect on the ozone layer diminishes.
While Chlorine compounds play a major role in the ozone depletion, they are definitely not the only cause. Currently research is being conducted into other trace substances with an effect on the stratospheric ozone concentrations, among them Bromine (Br) compounds, because Br and BrO can serve as even more potent catalysts in reactions (2.10) and (2.11). [Richter et al., 1999a]

The most distinct feature of ozone depletion in the stratosphere is the Antarctic "ozone hole". This is due to conditions with stratospheric clouds – their formation depending on aerosols, due to the small amounts of water present – in the Antarctic winter, allowing Chlorine to get out of its less reactive reservoirs and then cause the ozone depletion when photochemical activity returns with the sun during polar spring. The growing ozone hole has been observed every October since the late 1970s (see also figure 2.5 and the second picture in figure 2.7). Similar developments are being observed in the Arctic, but in a less pronounced manner.

Globally the ozone layer was observed to slightly reduce on longterm scale (see figure 2.6). For the northern mid latitudes decreases of total ozone in the magnitude of 1.2% to 2.7% per decade, depending on the season, have been observed. This resulted in the northern mid- and polar-latitude O_3 levels during the last two months of 1996 being 5% to 8% below the 1957-1970 averages. Most of this reduction takes place in the lower stratosphere. Similar trends are observed in southern latitudes. For tropical regions, however, no such trends in O_3 have been recorded. [Hobbs, 2000, Chapter 10.2]

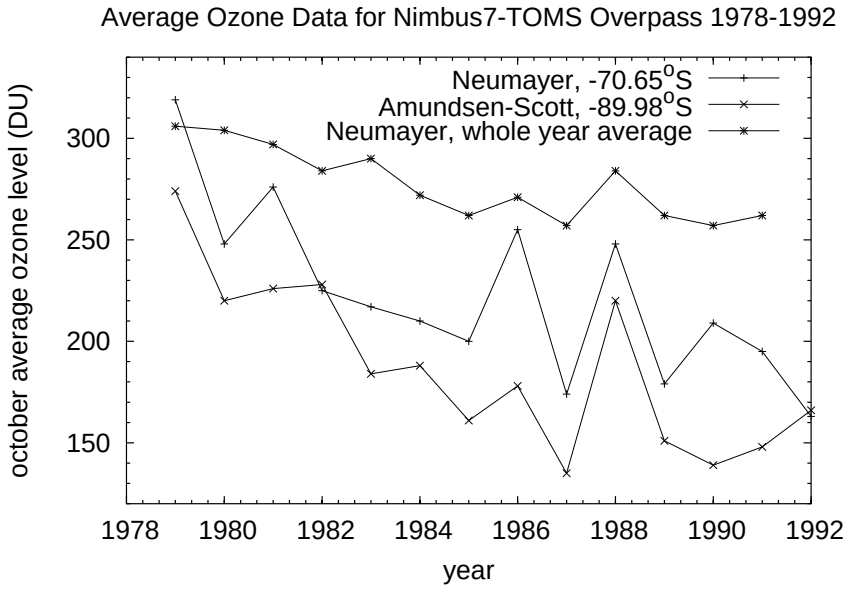

Figure 2.5: *Antarctic October ozone averages 1978-1992: Shown are averages of total column ozone during October measured by the Nimbus7-TOMS instrument over two Antarctic sites. For comparison the whole year average at one of the sites is shown. [Nimbus7-TOMS Data]*

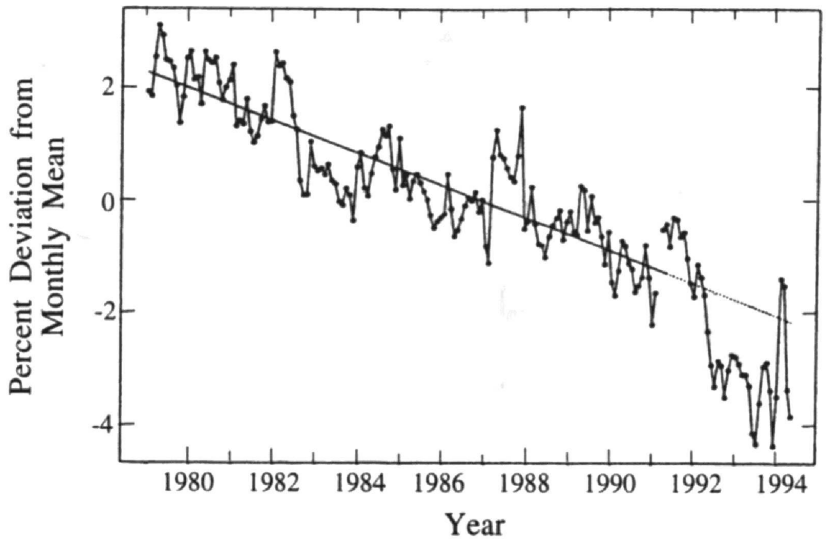

Figure 2.6: *Total column ozone (60°N to 60°S) from January 1979 to May 1994 measured by the solar backscattered ultraviolet spectrometer, SBUV (WMO, 1994). The solid line is a least squares fit to the data through May 1991. The dashed line is an extrapolation through May 1994. The annual cycle and the QBO have been removed. [Adupko, 2002]*

2.3 Ozone in the Tropics

After discovering the ozone hole phenomenon research on and monitoring of the ozone layer has focused on the polar regions. Therefore few permanent stations aquire regular ground-based measurements or sonde soundings in the tropics. As the atmosphere is a dynamical system, however, also the tropical region, located approximately between the Tropic of Cancer (23.5° N) and the Tropic of Capricorn (23.5° S), plays a key role in the global ozone chemistry.

The tropics play a crucial role for the stratospheric ozone layer as stratospheric ozone is produced photochemically, and because the incident radiation is strongest in the equatorial region, it is here that ozone production is highest. The reason for the peak concentrations to appear in polar and mid latitudes is meridional transport away from the equator. Figure 2.7 shows the global total ozone columns, i.e. mainly stratospheric ozone, as measured with the EP/TOMS instrument for March and October 2002. Around the equator the total amounts show less fluctuation, but are also generally lower (around 220-280 DU[3]) than in mid latitudes, where maxima are reached in the respective spring periods.

The air circulation around the equator is dominated by the intertropical convergence zone (ITCZ). Southerly and northerly air flows meet near the equator and here the warm tropical air rises. This actually makes it difficult for gases in the lower troposphere to mix across the equator. Therefore in this layer the ITCZ forms an effective barrier between the Northern and Southern Hemispheres, allowing trace gases to have very different concentrations. Obviously this is only the case for low altitudes.
A point where tropospheric air can easily reach the stratosphere is near the subtropical jetstreams at approximately 30 degrees latitude, where the tropopause can break down.

Because emissions from industrial areas and traffic are less in the tropics, due to the more developed countries being located in the mid latitudes, these don't play such a crucial role in the atmospheric chemistry, except for the big urban centers. However, there are several unique factors in the tropics which are believed to influence ozone levels. Very prominent, especially in Africa, is biomass burning. This mainly encompasses vegetation fires during the dry seasons, releasing large amounts of the O_3 precursors NO_x and CO into the boundary layer. Figure 2.8 shows the global and African fire distribution. This places the main region of African biomass burning in a belt south of the Sahara and north of the equator, stretching from Western Africa up to Northern Uganda and Kenya. This belt moves with the dry season as defined by the shifting ITCZ. A majority of these fires are actually not wildfires, but the result of agricultural waste burning as part of subsistence farming in a region of high grass production. The plumes from the fires are transported south-westerly by the wind, reaching far over the Atlantic ocean. As they rise upwards in the ITCZ, they then might even cross over to

[3]DU = Dobson Units, gives the thickness in 1/100 mm that a pure ozone layer would have at standard pressure and 0°C; 1 DU = 2.68×10^{16} molecules/cm^2

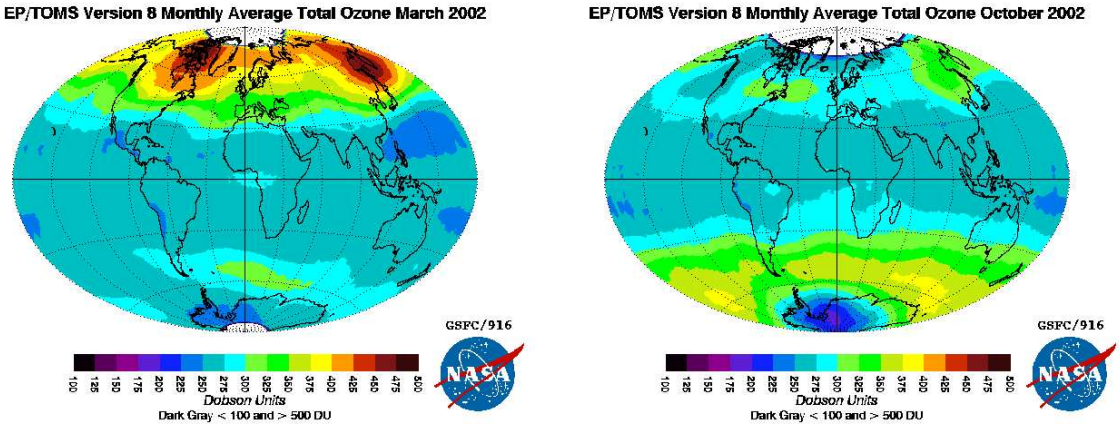

Figure 2.7: *Global total ozone columns measured with the EP/TOMS instrument. Monthly averages for March and October 2002. Tropical concentrations are lower and show less variation by location than in mid and high latitudes. The second picture also shows the ozone hole during Antarctic spring. (NASA/GSFC)*

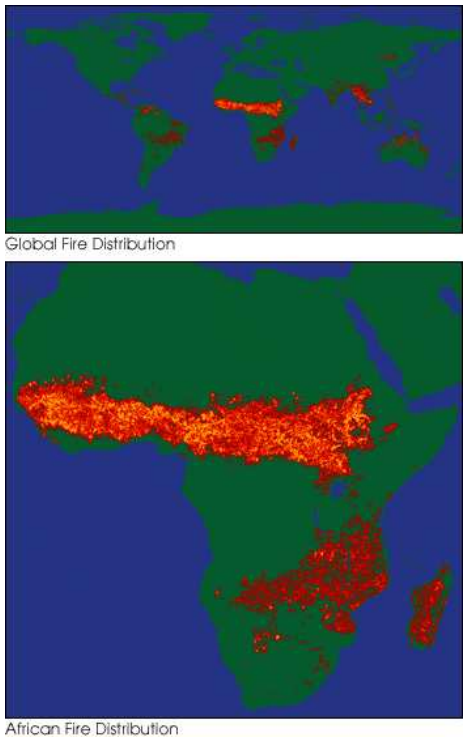

Figure 2.8: *Biomass burning: Global and African fire distribution. Africa is the fire center of our planet with more biomass burned on an annual basis than anywhere else. The upper image of the two shows the global distribution of fires, represented by red orange, and yellow dots (lighter colors indicate more fires), while the lower of the two images shows the fire distribution in Africa. They are both based on nighttime measurements obtained by the DMSP Operational Linescan System. (NASA/GSFC)*

the Southern Hemisphere [Edwards et al., 2003]. Another source for NO_x over Africa is lightning, which is actually believed to be the major source for NO_x in the mid-troposphere outside of the biomass burning season.

Periodic fluctuations of the global wind fields, like the Quasi-Biennial Oscillation (QBO) – having a period of approximately 28 months [Thompson et al., 2003b, and references therein] – or the El-Niño/Southern Oscillations (ENSO), can cause variations of up to five percent in stratospheric ozone amounts and influence tropospheric ozone columns (ENSO also influence tropospheric ozone when drought is followed by large fires). These phenomena occur in the tropical region.

3 Instruments and Measurement Techniques

Atmospheric ozone observations are usually performed in three different supplementary ways. The combination of the different techniques provides information about the processes governing ozone concentrations and the temporal development of these concentrations. They are also used to validate each other.

Ground-based stations using remote sensing techniques provide a high time resolution and document diurnal variations of atmospheric ozone; these include the classic Dobson spectrometers, as well as DOAS instruments. Usually, however, they can only measure total columns of ozone. MAX-DOAS is an attempt to partly overcome this shortcoming. There are worldwide networks of such stations and they are additionally used in campaigns aboard ships, aircraft or stratospheric balloons.

Satellite-based remote sensing instruments can provide global coverage on a daily or at least regular basis. They also yield only limited tropospheric and profile information, although a focus during the last decade has been in improving this data. A number of these instruments are described in section 3.3.

To make up for the lack of profile information from other measurements ozonesondes are launched with balloons at selected sites worldwide and during campaigns. They are especially useful in documenting transport processes of atmospheric ozone. However, they can neither give a good spatial nor temporal resolution.

Besides actually probing the atmosphere, scientists also develop models to calculate and simulate reaction and transport processes of trace gases in the atmosphere. The different measurements described here are also used to provide input and validate these atmospheric model calculations.

3.1 Differential Optical Absorption Spectroscopy

Hartley, after roughly measuring the absorption of ozone in the UV region (the Hartley band), suggested in 1880 that ozone was responsible for the absorption causing the sharp drop at the UV end of the solar spectrum, as received at the ground (see figure 3.1). Spectroscopical measurements of atmospheric ozone were carried out as early as 1920, first using spectral lines recorded on photographic plates. In the late 1920s Dobson developed a photoelectric spectrophotometer. The photoelectric cells used in the beginning were later replaced by photomultipliers. Otherwise, little has been changed in the setup of these instruments over the course of time. By observing narrow wavelength

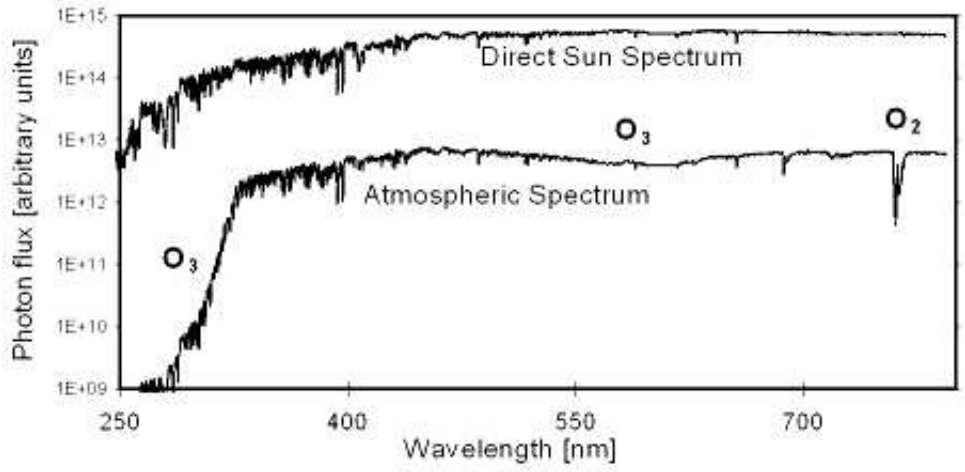

Figure 3.1: *Spectra of direct sun light and light reflected by the earth observed by the satellite instrument GOME on board the European research satellite ERS-2. (ESA, 1995)*

pairs (one located in and one outside of the O_3 Huggins absorption bands, see figure 3.2) total column ozone can be calculated relatively easily from their ratio and a geometrical factor (accounting for the solar zenith angle, SZA). Dobson Spectrometers are still in use today and have been providing long-term series of total column ozone for many locations around the world. [Dobson, 1968]

In the late 1970s the Differential Absorption Spectroscopy (DOAS) method was introduced by Noxon, Perner and Platt [Noxon, 1979; Perner and Platt, 1979]. DOAS basically relies on the absorption cross sections of atmospheric absorbers in suitable wavelength windows of the ultraviolet and visible region. Spectra of scattered sunlight are recorded and from the difference between these and a background spectrum, amounts of stratospheric absorbers along the light-path are quantified. Taking into account radiative transfer calculations these slant columns (SC) can be transformed into vertical columns (VC), i.e. total columns of the absorber density integrated over height. In this project passive DOAS using sunlight is covered. Measurements using moonlight have also been made with a slightly modified instrumental design.
Another application for the DOAS method is in using active systems with a spectrometer recording the light of a strong broadband lamp from a certain distance to determine the concentrations of absorbers in the light-path.

3.1.1 Experimental Setup

This section is dedicated to a description of the specific instrument used in this project, the Bremian MAX-DOAS (Multi-Axis DOAS). It was developed at the University of Bremen's Institute of Environmental Physics (IUP) and is now in use at different sites

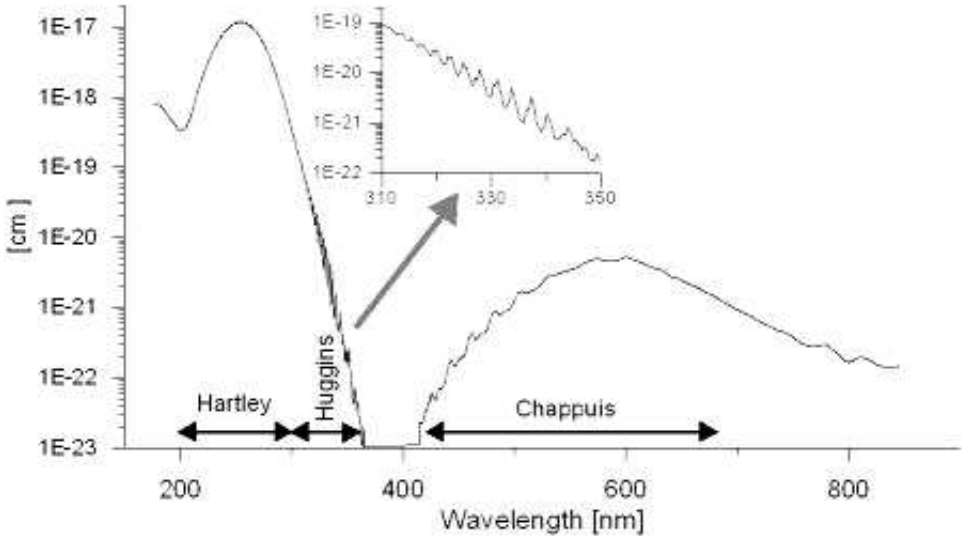

Figure 3.2: *O_3 absorption cross section. The highly structured O_3 Huggins Bands are also displayed in the insert graph with an expanded wavelength scale. They are often applied for atmospheric O_3 measurements. (IUP Heidelberg)*

of BREDOM (Bremian DOAS network for atmospheric measurements). BREDOM currently comprises instruments in Bremen, Germany (53°N, 9°E), Ny-Ålesund, Norway (79°N, 12°E), Mérida, Venezuela (8°N, 71°W), Summit, Greenland (72°N, 38°W) and Nairobi, Kenya (1°S, 37°E) – the location surveyed in this study.

The MAX-DOAS is a variation of the classic DOAS setup through the introduction of additional off-axis viewing directions close to the horizon. The main goal of this enhancement is a distinction between tropospheric and stratospheric absorption, i.e. determination of a rough vertical profile. A major application is in the validation of satellite based DOAS measurements (section 3.3), for which algorithms to distinguish between tropospheric and stratospheric absorption are under development.

The spectrographic instrument used for the DOAS measurements consists of a telescope to collect the sunlight, connected to a Czerny-Turner spectrometer through a quartz fiber bundle. The spectra are recorded by a charged coupled device (CCD) detector and saved on a computer that also controls the telescope and spectrometer. The instrumental setup is sketched in figure 3.3.a.

The Telescope

The telescope is housed in a watertight box and has two UV-transmitting quartz glass windows for zenith sky and near-horizon viewing directions. This box is shown (a) schematically and (b) as a photo in figure 3.4. A mirror mounted on a turntable can

be used to select a certain direction of the light coming through the off-axis window B and reflect it onto the opening F in the dividing wall (illustrated in figure 3.4.b). For zenith sky measurements the mirror is moved to the left into an upright position to block the light from the off-axis window and allow the light entering through window A to pass through. The light passing through the opening F then is focused by the lens G onto the mounting H for the quartz fiber bundle, as shown in figure 3.4.a. The bottom part of the telescope contains a calibration unit consisting of a mercury-cadmium lamp K and a tungsten lamp J, the first for wavelength calibration and the second to detect and compensate possible etalon effects. For calibration measurements, usually performed every night, the unit can be separated from the telescope by closing shutter E.

The quartz fiber bundle connecting the telescope box with the spectrometer, located indoors, consists of 38 cylindrical fibers, each of which has a diameter of 150 μm (plus 15 μm coating). At the mounting in the telescope the fibers are positioned discoidal, while at the other end at the entrance to the spectrometer they are aligned in a row to form the slit. If two spectrometers are connected to the telescope the fibers are divided evenly between them. Besides allowing to set up the telescope at some distance from the rest of the instrument, the quartz fibers function as depolarizer in the setup, minimizing any effects that would result from a polarization dependency of the instrument.

The Spectrometer

The spectrograph used for the MAX-DOAS instrument is of the Czerny-Turner type as outlined in figure 3.3.b. It consists of two convex mirrors and a plane diffraction grating, to spatially separate the light of different wavelengths before it is projected onto the CCD detector. The slit-forming quartz fibers are mounted in the focal point of the first convex (collimating) mirror. This mirror projects parallel light onto the grating, where it is dispersed. The second convex mirror is the focusing unit for the dispersed light onto the detector. The design is optimized to avoid any straylight that could, for example, result from the diffracted light reflecting from the mirrors back to the grating. This could cause unwanted additional noise in the measurements. The spectrometer is kept at a constant temperature of 35° Celsius to avoid changes to the setup that could result from a temperature fluctuation.

The CCD

As detector a back-illumination UV-enhanced Andor CCD is used. It is a silicon-based semiconductor chip with a two-dimensional matrix of photo-sensors (pixels). To reduce dark-current influences the CCD has to be kept at a low temperature of -35° or -40° Celsius. In a first version a shutter was used to close off the whole spectroscopical unit for reading out of the CCD. To ensure longtime stability independent of a functioning shutter this was later abandoned. Half of the input slit was covered and so only half of the CCD is illuminated, allowing to shift the charge to the non-illuminated part for readout.

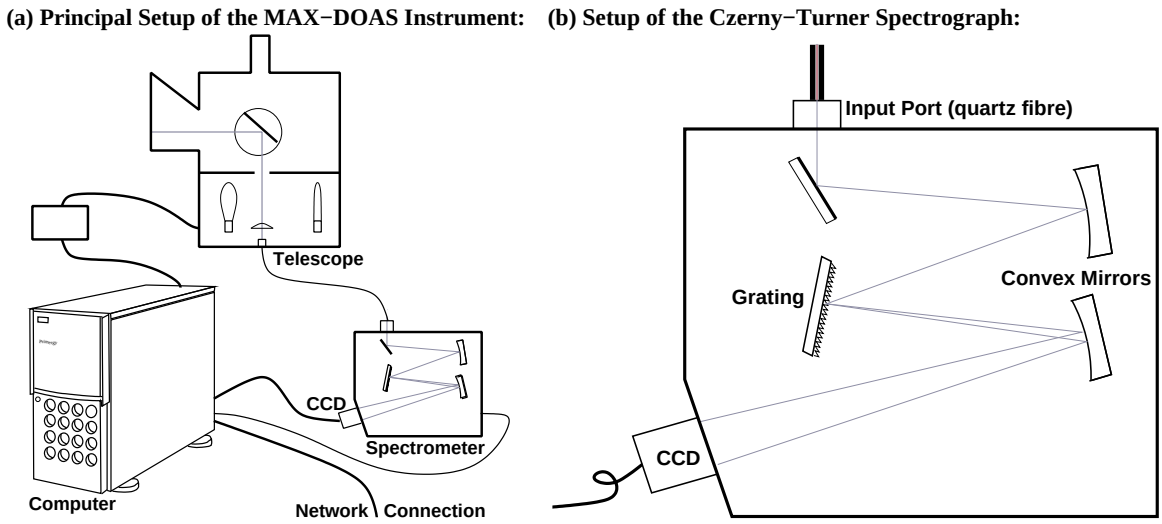

Figure 3.3: *Sketch of the instrumental setup and the Czerny-Turner spectrograph.*

The PC

Each CCD is connected to a computer for data recording. If there are two spectrometers in use, one of the PCs is acting as master for synchronization and to control the telescope (measurement angle, calibration, etc.), while the other is the slave for recording the second CCD. The software MAX-OMA, developed at the IUP Bremen, is used to save the data in binary files and control all the features. It also plots the current measurements on the screen. Once configured it governs everything in an automatic mode.

3.1.2 MAX-DOAS in Nairobi

The University of Bremen's ground-based DOAS station in Nairobi (1°S, 36°E) was installed in August 2002 at the headquarters of the United Nations Environmental Program (UNEP), located on the UN campus in Gigiri, north of Nairobi's city center. It is officially hosted by the UNEP's Ozone Secretariat. Because earlier measurements have focused on mid and high latitudes, the University of Bremen decided to extend its DOAS network to tropical stations. The high biomass burning activity in Africa was one of the factors leading to a decision for this continent. Nairobi was chosen, as Kenya has been politically stable compared to other African countries near the equator. In Nairobi the UNEP, besides working on ozone policy where the DOAS is indirectly contributing to monitoring efforts, could offer a secure power supply and internet connection, necessary for the continuous, remote administered operation of the station.

The instrument is basically the standard Bremian MAX-DOAS setup, as described above, with the telescope mounted on top of the outside stairs of one of the buildings and its off-axis window pointing to downtown Nairobi in the South, while the spectrometers and computers are located inside the building.

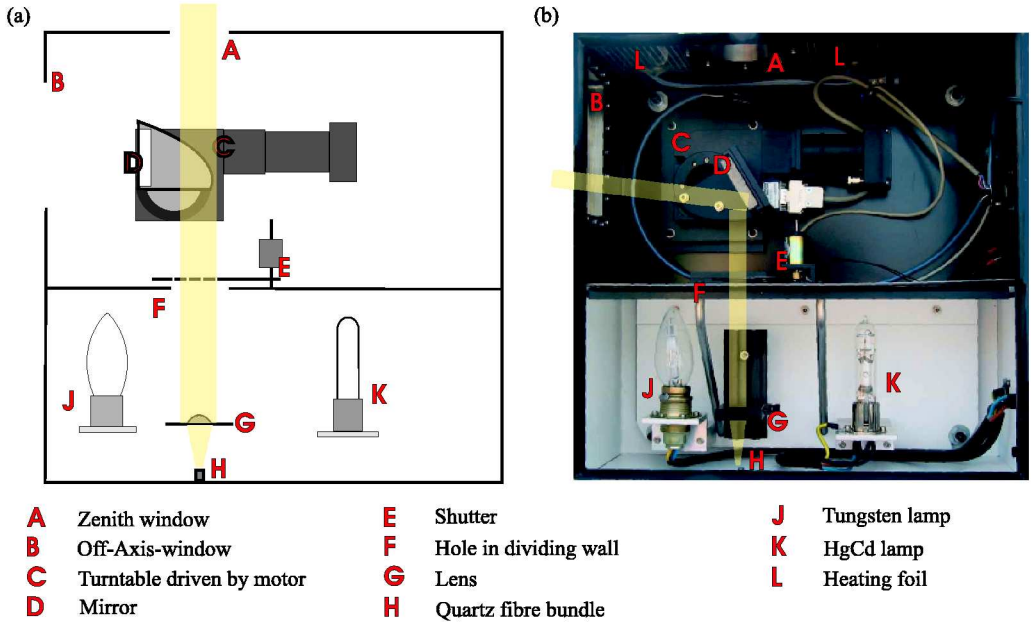

Figure 3.4: *Illustration of the MAX-DOAS entrance optic. The scheme on the left shows the position of the mirror for zenith sky observations, whereas the photo on the right was taken in the horizon viewing mode. (University of Bremen, IUP)*

Figure 3.5: *The telescope of the Nairobi MAX-DOAS instrument with off-axis directions facing ahead towards downtown. (University of Bremen, IUP)*

Table 3.1: *Specifications of the two spectrometers in Nairobi.*

UV range	**visible range**
operational since August 2002	operational since January 2004
Czerny-Turner Spectrograph L.O.T. MS257 focal length 257 mm 1200 l/mm grating	Czerny-Turner Spectrograph L.O.T. MS260i focal length 260 mm 600 l/mm grating
CCD Andor DV440-BU 2048 x 512 pixels pixel size: 13.5 μm active area: 27.6 x 6.9 mm^2 linearity: better than 1%	CCD Andor DV420-BU 1024 x 256 pixels pixel size: 26 μm active area: 26.6 x 6.6 mm^2
wavelength region 320-410 nm	wavelength region 395-565 nm
spectral resolution $\sim$ 0.55 nm	spectral resolution $\sim$ 0.9 nm

Different viewing directions can be achieved by moving a mirror on a turntable inside the telescope. In the automatic mode the computer continuously alternates between zenith sky observation (90°) and 4 horizontal off-axis directions (4°, 7°, 16° and 30°). Daily calibration measurements with the Tungsten lamp and the HgCd lamp are performed during nighttime.

After the instrument was initially built up with only one spectrometer in the UV range, a second spectrometer for the visible range was added in January 2004. The specifications of the two spectrometers can be seen in table 3.1. Each gets the input from half of the quartz fibers coming from the telescope.

3.2 The DOAS Technique

3.2.1 Retrieving Slant Columns

The following detailed description of the DOAS technique basically follows that of Richter [1997].

The basic equation underlying all absorption spectroscopical measurements is the **Lambert-Beer-Law**, stating that in a homogenous absorbing medium the intensity I of light is decreasing exponentially with the distance s travelled within the medium:

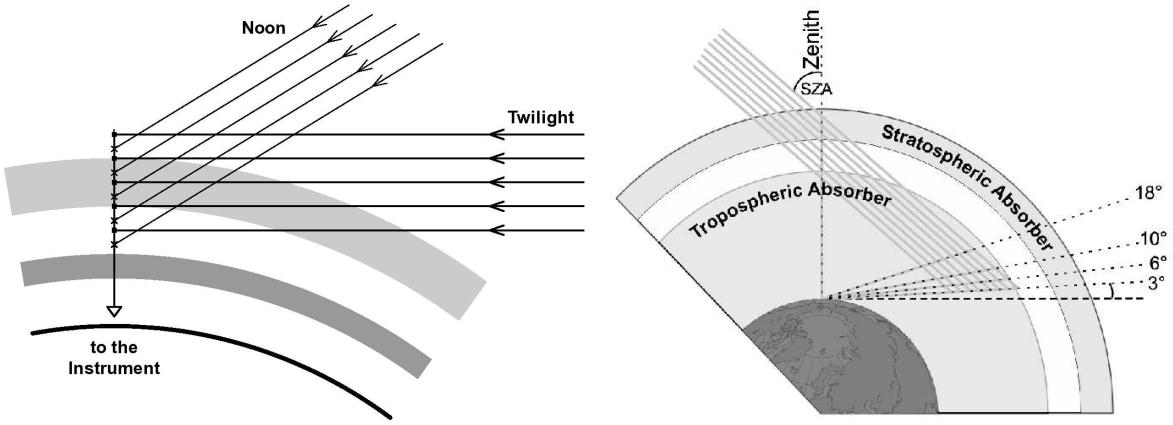

Figure 3.6: *Illustration of the zenith DOAS (left) and MAX-DOAS (right) geometry. For the classic setup most of the light-path is through the stratosphere, depending on the SZA. Horizon viewing observations have a similar path through the stratosphere, whereas the light path in the troposphere is extended and increases with decreasing elevation angle. [Richter, 1997; Wittrock et al., 2004]*

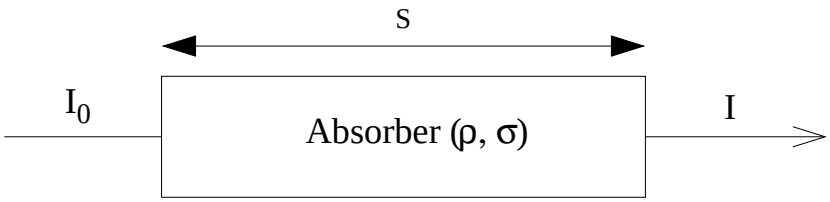

$$I(\lambda) = I_0(\lambda)e^{-s\rho\sigma(\lambda)} \tag{3.1}$$

where I_0 is the original intensity, λ the wavelength, ρ the particle density of the absorber and $\sigma(\lambda)$ its absorption cross section.

When looking at broadband absorption in the atmosphere, several absorbers with strong variations of their cross sections in the observed wavelength window have to be taken into account at the same time (for sample cross sections of some absorbers see figure 3.7). Their concentrations and cross sections are depending on the altitude, i.e. they are temperature and pressure dependent. For J absorbers this yields:

$$I(\lambda) = I_0(\lambda) \exp\left\{ -\int \sum_{j=1}^{J} \rho_j(s)\sigma_j(\lambda, s)ds \right\} \tag{3.2}$$

The integral is taken along the light-path through the atmosphere and depends on wavelength and solar-zenith angle (SZA).

Additionally atmospheric scattering processes by air molecules and aerosols have to be accounted for. This can be approximated by treating scattering as additional

weakening according to the Lambert-Beer-Law, where the cross section σ is replaced by scattering cross sections σ_{Ray} and σ_{Mie} for Rayleigh- and Mie-Scattering. Additionally rotational Raman-Scattering by air molecules, leading to the so called Ring Effect (the filling in of Fraunhofer lines [de Beek, 2001]), has to be considered. We can also approximate this as an additional effective absorber σ_{Ring}.

$$I(\lambda) = I_0(\lambda) \exp\left\{ -\int \left[\sum_j \rho_j(s)\sigma_j(\lambda, s) + \rho_{\mathrm{Ray}}(s)\sigma_{\mathrm{Ray}}(\lambda, s) \right.\right. \\ \left.\left. +\rho_{\mathrm{Mie}}(s)\sigma_{\mathrm{Mie}}(\lambda, s) + \rho_{\mathrm{Ring}}(s)\sigma_{\mathrm{Ring}}(\lambda, s) \right] ds \right\} \tag{3.3}$$

To simplify this equation the height dependence of the cross sections should be neglected. Thus it is possible to take the cross sections out of the integral and replace the path integral over the particle densities by the slant columns $\mathrm{SC}_j \equiv \int \rho_j(s) ds$. The Ring Effect will be treated as another absorber:

$$I(\lambda) = I_0(\lambda) \exp\left\{ -\sum_j \sigma_j(\lambda)\mathrm{SC}_j - \sigma_{\mathrm{Ray}}\mathrm{SC}_{\mathrm{Ray}} - \sigma_{\mathrm{Mie}}\mathrm{SC}_{\mathrm{Mie}} \right\} \tag{3.4}$$

Equation (3.4), however, does not yet allow to separate the individual processes. One problem is that clouds can change the intensity of the scattered light by a whole order of magnitude, completely covering the influence of trace gases, as they will at most cause absorptions of a few percent in the observed wavelength window. To account for this the cross sections are separated into a part which varies only slowly with the wavelength σ_j^0 and a rapidly varying part σ_j' called the differential cross section. This is one of the fundamental ideas of the DOAS technique accounted for by the "differential" in the name. It is usually realized by subtracting a low order polynomial from the cross sections as demonstrated in figure 3.8. The slowly varying components together with Rayleigh- and Mie-Scattering are approximated by a polynomial:

$$I(\lambda) = I_0(\lambda) \exp\left\{ -\sum_j \sigma_j'(\lambda)\mathrm{SC}_j - \sum_p a_p \lambda^p \right\} \tag{3.5}$$

This is possible as the cross sections for Rayleigh- and Mie-Scattering approximately follow the relations:

$$\sigma_{\mathrm{Ray}} \sim \lambda^{-4} \qquad \sigma_{\mathrm{Mie}} \sim \lambda^{-\kappa} \qquad \kappa = 0 \ldots 2$$

The application of this separation of cross section components is only possible for absorbers with a highly structured spectrum. The DOAS technique is therefore not feasible for absorbers for which no wavelength window with rapidly varying absorption cross section can be found. Ozone, however, has such a structure in the UV Hartley-Huggins Bands and the visible Chappuis Bands (figure 3.2) making it an ideal trace gas for observations with DOAS. Other observable gases include NO_2, BrO and OClO.

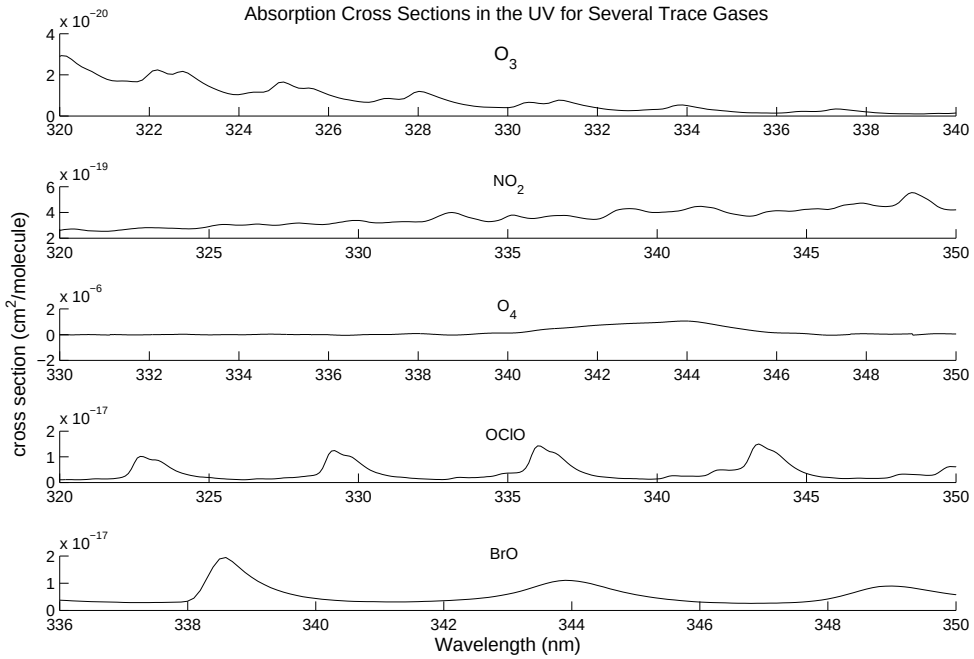

Figure 3.7: *Cross sections for different absorbers in the UV. DOAS is also commonly applied to measurements of light in the visible region.*

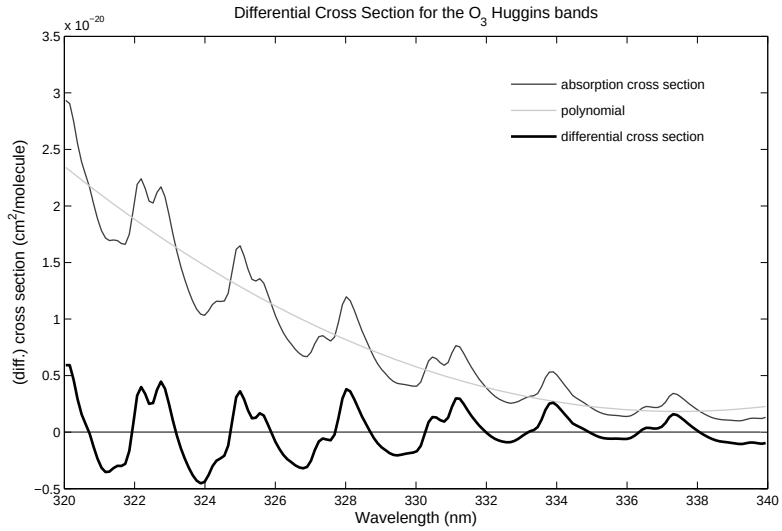

Figure 3.8: *Differential absorption cross section for the Huggins Bands of ozone. The upper part of the graph shows the original cross section and the fitted polynomial. Below the resulting differential cross section after substraction of the polynomial is shown.*

Finally to analyse the measurements the logarithm of the measured spectrum is taken:

$$\ln I(\lambda) = \ln I_0(\lambda) - \sum_j \sigma'_j(\lambda)\mathrm{SC}_j - \sum_p a_p\lambda^p \tag{3.6}$$

The required slant columns SC_j and polynomial coefficients can be calculated in a suitable wavelength interval through a linear compensation calculation from this equation. Therefore (3.6) is called the **DOAS equation**.

Reference Spectrum

For the selection of a reference spectrum I_0 for atmospheric measurements we have two possibilities: (1) To take an extraterrestrial sun-spectrum, for example measured from satellite instruments (GOME, see section 3.3.2, was the first instrument to yield such spectra with a suitable resolution). (2) To take a "noon" spectrum, i.e. smallest possible SZA, measured with the same instrument, preferably on the same day.
Usually the second procedure is applied, as it automatically cancels out instrumental features which otherwise would have to be taken into account. This actually is the only way to detect weak absorbers like BrO with simple experimental setups.

The disadvantage of an atmospheric reference spectrum I_0^A is that actually only the difference between the slant columns of both measurements is retrieved from the ratio I/I_0^A:

$$\ln \frac{I_0^A(\lambda)}{I(\lambda)} = \sum_j \sigma'_j(\lambda)(\mathrm{SC}_j - \mathrm{SC}_j^A) + \sum_p a_p\lambda^p \tag{3.7}$$

Therefore additional considerations are required when calculating the vertical columns (VC). This will be described in section 3.2.2.

Correction of Fraunhofer lines

Before evaluating measurements with the DOAS equation (3.6), a correction for the Fraunhofer lines has to be applied. The sun sends out black body radiation, but absorptions in the sun's atmosphere account for highly varying structures in its spectrum, known as Fraunhofer lines. These can be two orders of magnitude above the absorption structures in the earth's atmosphere that the DOAS is supposed to detect and therefore require a correction. For zenith sky observations and an atmospheric reference spectrum the influence should cancel out during the calculation; however, already a slight misalignment between the wavelength axes can lead to large residuals in the fittings and considerable errors in the results. To account for this, the wavelength axis is varied slightly in an iterative process during the evaluation of the data and the result with the smallest residual for the DOAS fit is taken.

3.2.2 Conversion to Vertical Columns

The light-path through the atmosphere depends considerably on the time of day, i.e. the sun's position. For the DOAS with different viewing directions, as described below, additional considerations have to be made concerning the path through the atmosphere. The light-path through the atmosphere is accounted for by employing radiative transfer models (RTM). The RTM are used to calculate the so-called air mass factors (AMF) which are necessary to convert the slant columns into vertical columns. The AMF for an absorber j is defined as the quotient between SC and VC and is dependent on the wavelength λ and the zenith angle Θ:

$$\mathrm{AMF}_j(\lambda, \Theta) \equiv \frac{\mathrm{SC}_j(\lambda, \Theta)}{\mathrm{VC}_j} \tag{3.8}$$

This means that the **air mass factor** effectively indicates by how much the absorption along the actual light-path is greater than it would be along the vertical column.

The AMF are calculated (numerically) using a radiative transfer model. One such model developed at the University of Bremen is GOMETRAN which handels the atmosphere in a plane parallel approximation and was developed for the satellite project GOME [Rozanov et al., 1997]. An extension for the simulation of a spherical planetary atmosphere is SCIATRAN [Rozanov et al., 2001]. To calculate air mass factors the models solve the radiative transfer equation twice: Once with the selected absorber I_{+j} and once without I_{-j}. From this the AMF is obtained by the following equation:

$$\mathrm{AMF}_j(\lambda) = \frac{\ln(I_{+j}(\lambda)/I_{-j}(\lambda))}{\mathrm{VOD}_j(\lambda)} \tag{3.9}$$

where $\mathrm{VOD} \equiv \int_0^{z_0} \rho_j(z)\sigma_j(\lambda, z)dz$ is the vertical optical depth of the whole atmosphere for the absorber j. For this calculation the assumption of an optically thin atmosphere is made, i.e. the light-paths with and without absorber have to be equal. This works fine in the visible region, but tends to be not as accurate for the UV. A workaround for ozone in the UV is described below as "enhanced DOAS".

The DOAS technique can be applied independent of the measurement geometry, which, however, then has to be considered during the AMF calculation as the light-path through the atmosphere depends on the geometry of the instrument. The classic setup for atmospheric measurements are zenith sky measurements (90° elevation angle), as pioneered already by Dobson. Here the light-path and therefore the AMF strongly depend on the solar-zenith angle, as the light-path is considerably longer for bigger SZA (close to the horizon). In this study an instrument with additional viewing directions near the horizon was used. A more detailed description of this so called MAX-DOAS can be found in section 3.1.1; an illustration of the viewing geometry is given in figure 3.6.

Radiative transfer models depend on climatological input data. Besides temperature and pressure profiles of the atmosphere, information on aerosols and the mixing ratios

of the relevant absorbers is also necessary for the location under consideration. In the optimal case data from nearby sonde launches is used, but if this is not available and for altitudes above the burst height of the balloons, data from atmospheric models has to be taken.

For reasons of simplification many RTM only consider single scattering of the photons in the atmosphere. This way the light-path can be simply divided into two parts, before and after scattering. In reality, however, multiple scattering takes place in the atmosphere (by molecules, aerosols and water drops of clouds), which can considerably lengthen the light-path in the atmosphere, especially at low SZA. Therefore some RTM were extended to consider multiple scattering processes and as expected larger AMF and consequently smaller total columns for the absorbers were retrieved by this method. However, comparison with other data showed that in most cases the single scattering assumption yielded more realistic absorber columns. This phenomenon is still not clearly explained [Richter, 1997]. As a result AMF and optical depths based on single scattering were used in this study.

Enhanced DOAS

To account for the strong wavelength dependence of the AMF for ozone at short wavelengths (UV region), a result of the strong temperature dependence of the ozone cross section and a correlation between the AMF and the cross section in this region, the concept of enhanced DOAS was developed. Basically a synthetic spectrum for ozone in the UV is created for the site of measurement to serve as a basis for the DOAS fit. This spectrum already contains information about the optical depth (OD) and the fit directly produces vertical columns – therefore this method is also called OD-Fit.

To implement this method the slant columns (SC_j) of the absorbers in equation (3.4) are replaced by the slant optical depths (SOD_j):

$$I(\lambda) = I_0(\lambda) \exp\Big\{ -\sum_j \mathrm{SOD}_j(\lambda,\Theta) - \sigma_{\mathrm{Ray}}(\lambda)\mathrm{SC}_{\mathrm{Ray}} - \sigma_{\mathrm{Mie}}(\lambda)\mathrm{SC}_{\mathrm{Mie}} - \sigma_{\mathrm{Ring}}(\lambda)\mathrm{SC}_{\mathrm{Ring}} \Big\} \tag{3.10}$$

Afterwards the procedure is analogous to the standard DOAS algorithm: Transition to differential SOD and approximation of scattering and slowly varying components through a polynomial.

Like the AMF, the SOD are calculated using radiative transfer models. They then replace the cross section in the fit and instead of slant columns the fit yields the scaling factors for the deviation of the actual column from that in the model atmosphere used in the RTM. Through normalization of the SOD with the absorber columns of the model, the procedure directly calculates vertical columns as scaling factors.

Richter [1997] established that this method mainly yields improvements in the results when applied for ozone in the UV. This effect is less for visible wavelengths, where the temperature dependence of ozone is reduced. Also the application of OD-Fits to several absorbers, besides ozone, does not bring any further improvement in the results. The method is, however, only applicable for zenith sky measurements.

For the retrieval of ozone columns in this study OD-Fits with a single scattering assumption for the UV-wavelength window 332–339 nm were applied. The OD-Spectra were calculated at IUP Bremen with SCIATRAN using climatological input from the MPI-2D-Climatology (Max Planck Institut für Chemie, Mainz).

3.2.3 Off-Axis Measurements

The innovation to use DOAS instruments also for measurements close to the horizon and not only in the zenith sky setup was introduced in the early 1990s to continue observations in Antarctica as far into the polar night as possible [Sanders et al, 1993]. As the sun does not get very high during this time the light intensity and with it the signal-to-noise ratio is greatly improved using off-axis measurements. Sander's study showed that tropospheric absorption is much stronger for close to horizon observations, while absorbers predominantly located in the stratosphere don't show much difference when varying the viewing geometry. Radiative transfer models at this time could not calculate air mass factors for the light-path of off-axis viewing, therefore, the measurements had to be treated in a quantitative way.

For classic zenith sky measurements the light-path is mostly within the stratosphere, also for changing SZA angles. Therefore, the slant columns for stratospheric absorbers are much greater during early and late hours than at noon. This has been used for a long time in the so called "Umkehr Method" to get a rough vertical profile of stratospheric absorbers as conclusion from the most likely scattering height for different SZA.

Off-axis directions close to the horizon have a much higher sensitivity to tropospheric absorbers than the zenith sky measurements, because in this viewing mode the light-path through the troposphere is considerably longer than for zenith sky observations. Recently this fact has been used to separate tropospheric from stratospheric columns in ground-based measurements. The geometry is shown in figure 3.6. For the geometry in zenith viewing only the solar zenith angle (SZA) is of importance, in contrast to off-axis modes, where also the relative azimuth, which is the azimuth angle between the direction of the sun and that of the telescope, has to be considered for the calculations of the light-path. The elevation angle of the telescope is given as angle above a tangential plane to the earth's surface, i.e. for the zenith it is 90°.

The radiative transfer models have been improved so far nowadays, as to allow calculations of air mass factors for different viewing directions and thus made it possible to separate tropospheric and stratospheric absorber columns. At first, this feature was

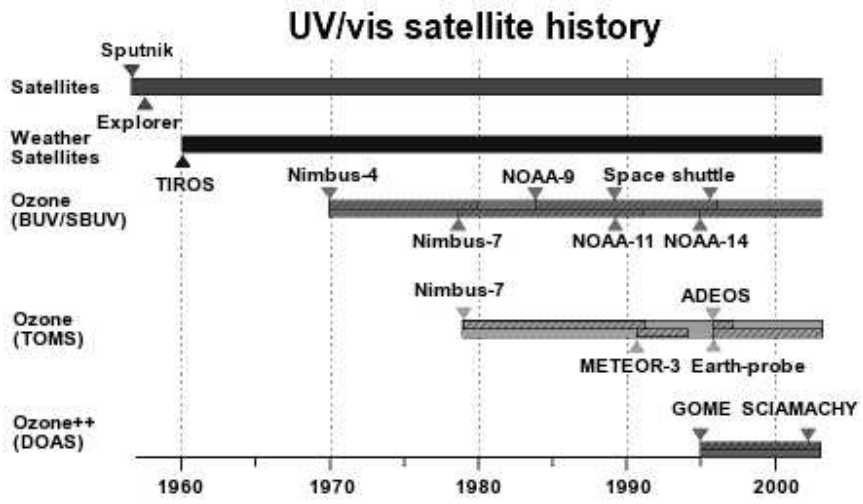

Figure 3.9: *Overview of the history of satellites carrying UV/vis sensors for ozone. (University of Heidelberg, IUP)*

not implemented routinely in the evaluation programs and could only be derived for single days at a time by assuming different vertical profiles in the AMF calculation and finding the one which gives the best agreement of vertical columns when converting the slant columns from the various viewing directions [Adupko, 2002; Wittrock et al., 2004]. Recently a retrieval for tropospheric columns was written at the IUP Bremen and so far seems to work well [S. Fietkau, private communication].

3.3 Satellite Based Instruments

Satellite based measurements of ozone have been going on since the 1970s, giving global coverage of total column ozone. Here, like with ground-based measurements, early instruments were using certain distinct absorption lines (similar to the Dobson spectrometers), while a new generation is now based on the DOAS technique. For the history of satellite based ozone measurements see figure 3.9.

3.3.1 TOMS

With the first research satellites only imaging devices were sent to space, producing pictures of the earth's surface and atmosphere. These visible and infrared images are still used in weather forecasting nowadays. First spectroscopical measurements in the UV and visible were carried out by the solar backscattered ultraviolet (SBUV) instrument aboard the American Nimbus-4 satellite. Like Dobson spectrometers this instrument was using a number of distinguished wavelength intervals for calculation of ozone columns. Observation of wavelengths with different penetration depths into the atmosphere yields

information about the vertical ozone profile. However, as these measurements suffered from instrumental instabilities NASA's first total ozone mapping spectrometer (TOMS) aboard Nimbus-7 allowed for more reliable remote sensing of the earth's atmosphere. Due to TOMS' use of longer wavelengths (see figure 3.10) it is not sensitive to the vertical distribution of ozone. Nimbus-7 has produced the so far longest global data set on ozone. Its successor concerning TOMS measurements, the Meteor 3 satellite, failed after only 3 years of operation and an almost 2 year gap of data occurred. Since 1996 EP/TOMS (Earthprobe TOMS) has again been able to give a continuous record.

The earthprobe satellite, with no other instruments besides the TOMS aboard, was launched in July 1996 and put into a sun-synchronous orbit at 500 km altitude with 11:16am local equator crossing time. After another TOMS instrument, launched a few months later, was lost with the failure of the Japanese meteorological satellite ADEOS, the orbit of EP/TOMS was raised to 739 km during December 1997, resulting in a two weeks gap in the measurements. This was done to receive a better daily global coverage of 90% (84% at equator and 100% at 30° latitude) at the expense of the resolution of the measurements. [McPeters et al., 1998]

EP/TOMS measures solar irradiance and the radiance backscattered by the earth's atmosphere in six selected wavelength bands in the ultraviolet. Using a mirror it scans the earth in 3-degree steps to 51 degrees on each side of the subsatellite point in a direction perpendicular to the orbital plane, which results in a ground-pixel size of 50×50 km^2 since the orbit was raised. These measurements are then used as the input for the algorithm to calculate total column ozone.

Possible uncertainties in the total columns of ozone measured and calculated from TOMS can have three origins: the accuracy and precision of the measurements, the value of the radiances calculated from the radiative transfer model, and the process of comparing the measured and calculated radiances to derive ozone. For EP/TOMS total ozone, the absolute error was determined to be ± 3%, the random error ± 2% and the drift after 1.5 years of operation was less than ± 0.6%. A comparison of EP/TOMS measurements with a network of 30 Dobson spectrometers showed the data to be consistent with these uncertainties, the EP/TOMS ozone being approximately 1% above the ground-based measurements.

The TOMS measurements are to be supplemented and continued in the future by the Dutch/Finish OMI (Ozone Monitoring Instrument) aboard the American EOS/Aura (Earth Observation System – Aura) mission launched in 2004. This instrument is supposed to combine advantages of both GOME/SCIAMACHY (sections 3.3.2 and 3.3.3) and the TOMS instrument and offer daily global coverage at a very high resolution (with ground-pixel size of 13×24 km^2). OMI-Data has, however, yet to be released.

In this study EP-TOMS version 8 archive overpass ozone data for Nairobi (1.27°S, 36.8°E) was used. [EP-TOMS Data]

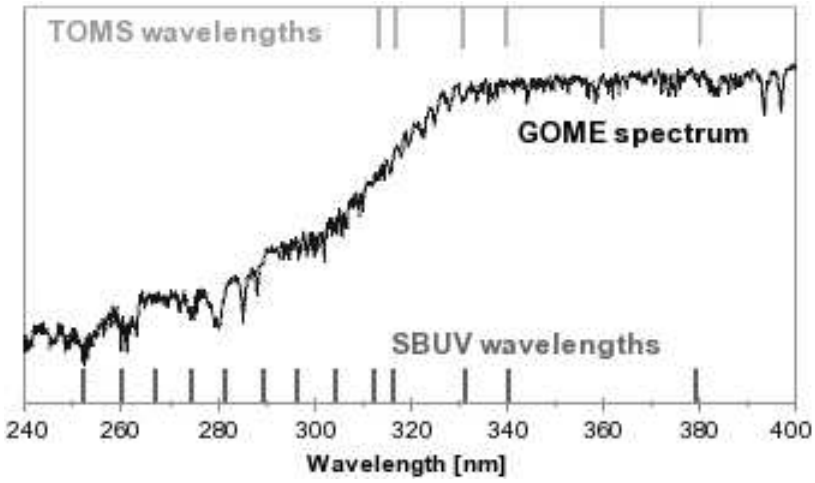

Figure 3.10: *The first O_3 sensors from space measured the reflected solar intensity in specific narrow wavelength intervals. For O_3 profile measurements the intensities at short wavelengths are observed (BUV/SBUV instruments); for the determination of the total atmospheric O_3 column the intensities at larger wavelengths are used (TOMS instruments). (University of Heidelberg, IUP)*

3.3.2 GOME

A new generation of space-borne ozone measuring instruments was introduced with the launch of the Global Ozone Monitoring Experiment (GOME) aboard the European Space Agency (ESA) Second European Remote Sensing Satellite (ERS-2), which was launched in April 1995. ERS-2 flies a sun-synchronous polar orbit at an average altitude of 785 km above the earth's surface with 10:30am local equator crossing time. The GOME spectrometer covers the UV and visible wavelength region and therefore allows the application of DOAS algorithms to determine columns of different atmospheric trace gases. [Burrows et al., 1999a,b]

GOME is a four-channel grating spectrometer measuring the sunlight scattered from the earth's atmosphere and/or reflected by the surface in nadir viewing mode in the spectral region between 240 and 790 nm at a moderate spectral resolution of between 0.2 and 0.4 nm (see figure 3.11). With an across track swath width of 960 km it reaches a spatial resolution of 40 $\times$ 320 km^2 ground-pixels and this results in global coverage being achieved after 3 days during 43 orbits.

The main objective of GOME is to monitor the ozone layer, but its broad spectral coverage allows to retrieve a lot more information; mainly in measuring columns of other trace gases, among them some of the key players in ozone chemistry, such as NO_2, BrO, H_2, O_4, O_2, NO_3, OClO and ClO.

The retrieval accuracy of the ozone slant columns is of the order of 1%. For ozone total (vertical) columns an additional uncertainty stems from the AMF calculation, which in conservative estimates is given as 5%. After improvements in the AMF calculations an agreement of ±4% was found for extensive comparisons to ground-based measurements.

3.3.3 SCIAMACHY

An improved European DOAS satellite instrument, the Scanning Imaging Absorption Spectrometer for Atmospheric Chartography (SCIAMACHY), was launched in early 2002 aboard ESA's ENVISAT satellite. GOME was actually first conceived as SCIAmini and constructed as a small-scale version of SCIAMACHY, launched to test the feasibility of the measurement concept and to aquire data while the bigger instrument was still under development. [Borrell et al., 2003]

SCIAMACHY mainly provides better spatial resolution for nadir-measurements with a ground-pixel size 15% of that of GOME (about 30 × 60 km^2), while extending the wavelength range into the near infrared (NIR) covering 240 nm to 2380 nm using 8 channels. Spectral resolution is between 0.24 and 1.58 nm depending on the channel. Figure 3.11 shows the wavelength coverage of SCIAMACHY, as well as the position of spectral windows where atmospheric constituents are to be retrieved. This also includes the absorptions of several greenhouse gases. The higher spatial resolution is particularly important for tropospheric constituents which show strong spatial gradients.

ENVISAT is on a sun-synchronous orbit at 800 km altitude with 10:00am local equator crossing time. The satellite has a 35 days repeat cycle of its orbits, but global coverage at the equator is reached after six days. [Bovensmann et al., 1999]

For the future several GOME-2 instruments are planned to provide even better spatial resolution.

3.4 SHADOZ – Ozone Sondes

The Southern Hemisphere Additional Ozonesondes (SHADOZ) network was introduced by NASA's Goddard Space Flight Center (GSFC) with international partners in 1998 to address the lack of continuous profile data for the tropical and subtropical region, especially on the Southern Hemisphere [Thompson et al., 2003a,b]. Earlier most measurements had been sporadic or campaign-based, but observations of long-term trends are necessary for many applications. SHADOZ aims to augment ozone balloon launches at operational sites on a cost-share basis with international partners to ensure continuous data acquisition, while making the data quickly and widely available through a

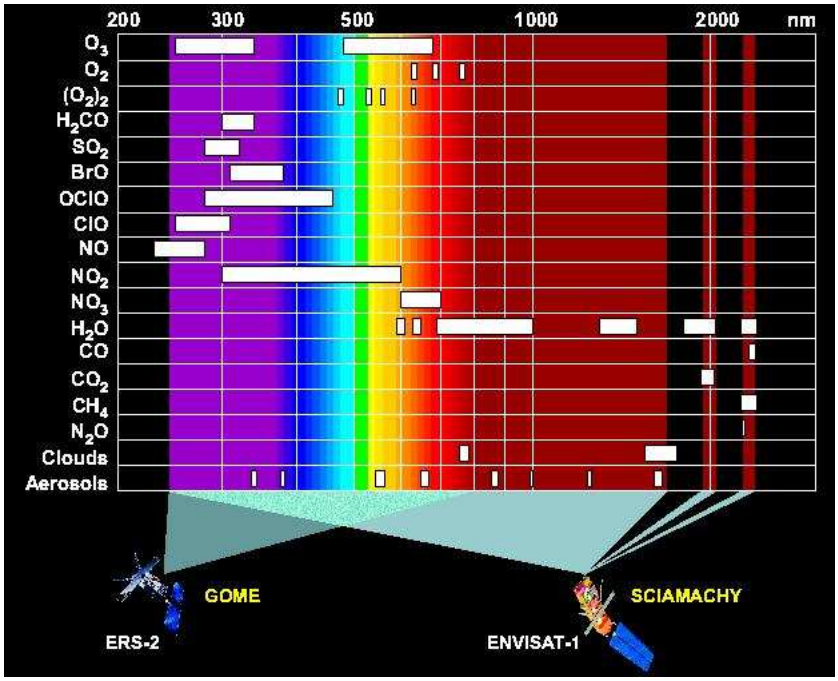

Figure 3.11: *Spectral coverage of GOME and SCIAMACHY. SCIAMACHY includes also the near IR with the absorptions of CO, CO2, CH4, and N2O. (University of Bremen, IUP)*

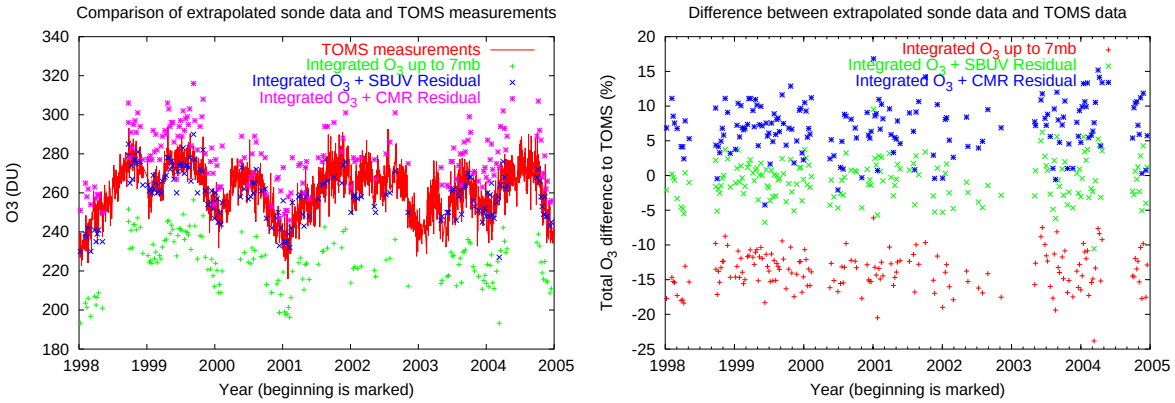

Figure 3.12: *Comparison of extrapolated sonde data and TOMS measurements. The absolute differences and percental deviations for integrated sonde ozone columns, as well as extrapolated total columns using the SBUV Residual and the Constant Mixing Ratio (CMR) Residual methods are shown. [SHADOZ Ozonesonde Data; EP-TOMS Data]*

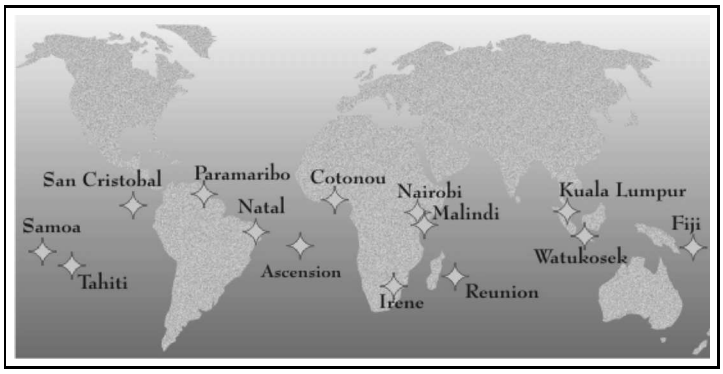

Figure 3.13: *Stations of the SHADOZ network. (GSFC)*

central database on GSFC webservers. The network currently comprises of 14 stations as shown in figure 3.13.

Sampling at all stations is once-per-week or at least forthnightly, usually, but not always, midweek and during the morning hours. Balloon-borne ozonesondes (electrochemical concentration cells, ECC) are coupled with a standard radiosonde for data telemetry; transmitting air pressure, air and pump temperatures, relative humidity, and ozone concentrations to a receiving station on the ground. The balloons can reach up to an altitude of approximately 40 km, but sometimes burst prematurely. For a typical ozone and temperature profile received by the ozonesondes above Nairobi refer to figure 2.1.

To receive total columns of ozone the measured data has to be integrated and extrapolated for above-burst ozone, for example assuming a constant ozone mixing ratio from the burst-point upwards or using SBUV-profiles. This extrapolation is in the end one of the main uncertainties in measurements, besides the fact that each launch carries a new instrument. Nairobi is actually one of the stations with the best agreement between extrapolated sonde ozone columns (using SBUV-profiles) and TOMS ozone columns: this agreement is within 5%. Assuming a constant mixing ratio generally gives a too high total ozone column of up to 12% above TOMS measurements (see figure 3.12).

Ozonesonde data from the SHADOZ network Nairobi station (1.27°S, 36.8°E, elevation 1795m) was used in this project. Near Nairobi sonde launches have been carried out on a weekly basis since 1998 by the Kenya Meteorological Department (KMD) in cooperation with the Swiss Meteorological Agency. [SHADOZ Ozonesonde Data]

4 Analysis and Discussion

4.1 Data Analysis

To calculate the ozone columns above Nairobi from the MAX-DOAS measurements the appropriate software developed at the IUP-Bremen was used. Figure 4.1 shows a schematic representation of the data evaluation process and programs used. The automated measurements taken by the Experimental Setup described in section 3.1.1 are coordinated and recorded by the software MAX-OMA on the computers at the measurement site. This yields daily binary files for every viewing direction and for the calibration measurements of that day. To calibrate the spectra (alignment of the wavelength axes with the help of the line spectrum, etc.) and calculate the slit functions the programs NPREPARE and RESOLUT are used respectively.
These calibrated spectra are now in the necessary format to use them as input for the DOAS-Fit performed by the program NLIN_D. Additional input are the absorption cross sections of the absorbers and a cross section to account for the Ring Effect. The calculations of this and the other programs are governed by parameter files saved in a plain-text format. For NLIN_D the parameter file contains information such as the wavelength window used in the fit, the absorbers examined and days and viewing directions considered. Another important option is the reference spectrum chosen for the fit. The tool NVERT allows to calculate vertical columns from slant columns using the air mass factors and selects a.m. and p.m. values of measurements for every day of the chosen month. With the help of the programs WINSPEC, MULTSPEC and SHOWFIT the input and output data can be visualized at different points during the process.

The satellite and sonde data used in this study were acquired in a readily processed form. For the SHADOZ ozonesondes and EP/TOMS overpass ozone this data can be downloaded via Internet from the NASA-GSFC [EP-TOMS Data; SHADOZ Ozonesonde Data]. Processed GOME and SCIAMACHY data for the relevant time period was provided by the IUP-Bremen.

4.2 Comparison of the Different Data Sets

4.2.1 Ozone Fit in the UV Versus Visible

For Nairobi UV spectral measurements are available continuously since August 2002. Visible measurements are available for the period between January and August 2004 (after which the PC for this instrument failed and measurements were only resumed in April 2005).

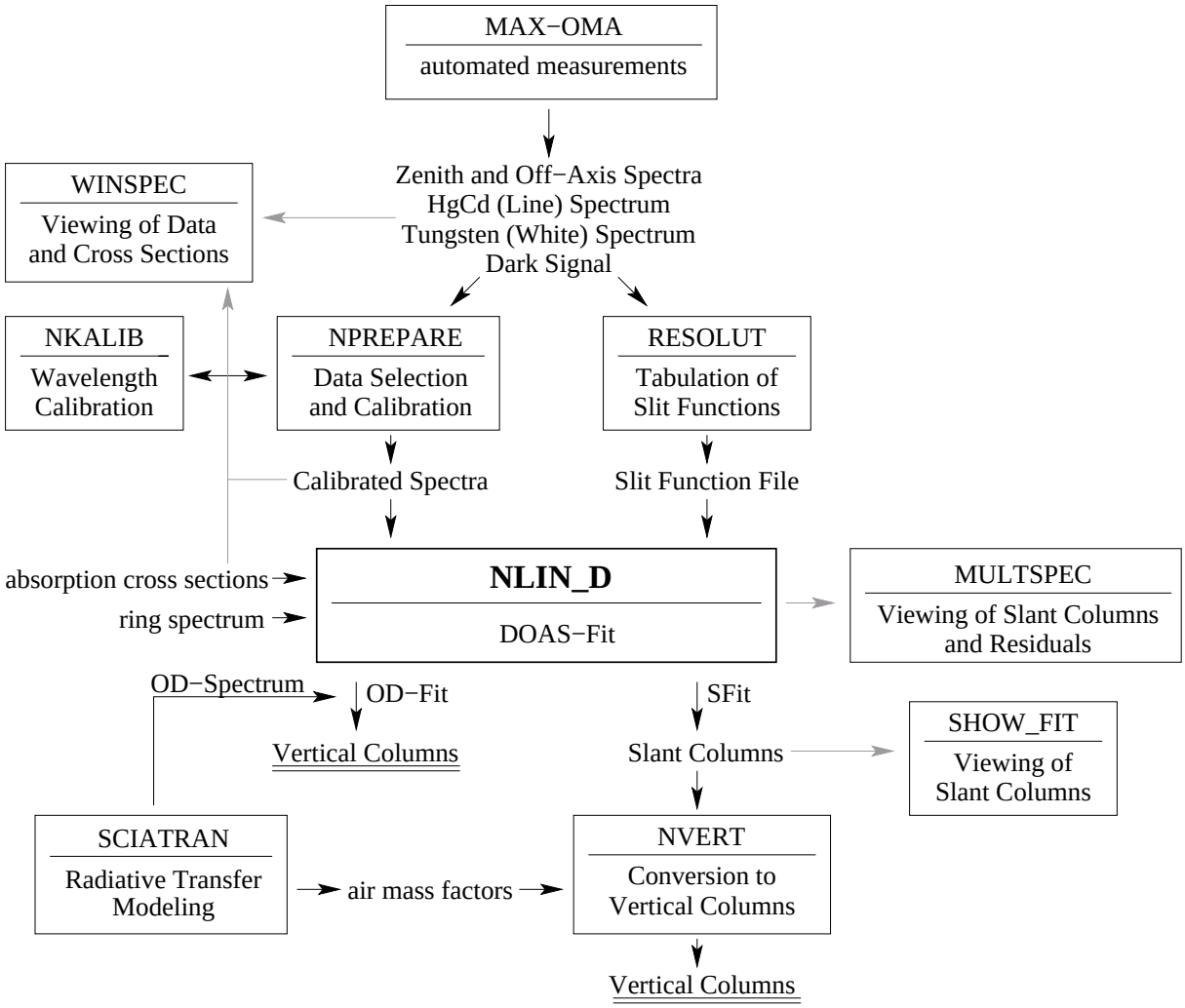

Figure 4.1: *Schematic representation of the data evaluation of ground-based DOAS measurements using the IUP-Bremen software.*

In both wavelength regions ozone has a distinct enough absorption cross-section to allow the successful application of a DOAS fit. Therefore a comparison was made. Where not mentioned otherwise the spectral data from the zenith-sky viewing direction was used.

In the UV region fitting was done using the "enhanced DOAS" method described above, directly yielding vertical ozone columns, as the conversion factor from slant columns is included into the cross section. To account for the temperature dependence of the O_3 absorption cross section a second cross section taken at a different temperature is also fitted. Parameters for this fit are summarized in table 4.1:

Table 4.1: *Parameters used for the OD-Fit of ozone in the UV region.*

wavelength window:	330 – 336 nm
fitted absorbers:	O_3, NO_2 (at 223K), Ring-Spectrum
background spectrum:	same day noon spectrum (21° SZA)
scattering:	single scattering OD-Spectrum for O_3

In the visible region the OD-fitting method is not applicable and therefore a classic DOAS fit (SFit) was performed and the slant columns then converted to vertical columns using the SCIATRAN air mass factors provided by the IUP Bremen. Parameters for this fit are summarized in table 4.2:

Table 4.2: *Parameters used for the SFit of ozone in the visible region.*

wavelength window:	447 – 493 nm
fitted absorbers:	O_3 (at 221k), NO_2 (at 221K), O_4, H_2O, Ring-Spectrum
background spectrum:	same day noon spectrum (smallest available SZA)

Data was selected using the tool NVERT (which also does the conversion to vertical columns). Morning (a.m.) and afternoon (p.m.) values were selected by averaging measurements taken at SZA between 80° and 85° with a fitting error of not more than 5%. For Nairobi this usually means that measurements from around 7am and 6pm are being evaluated. In figure 4.2 the a.m. and p.m. values were plotted together with EP/TOMS measurements as reference. TOMS has been measuring continuously for many years and its measurements are well validated and show no major deviation from the global Dobson network. The period shown is the complete period for which measurements of the visible spectrograph were available.

The comparison shows that for a.m. as well as p.m. data the values from the visible fit show a higher short term fluctuation than those from the UV fit: It is around 20 DU for the visible and around 10 DU for UV. Also the UV data agrees better with TOMS in absolute values as well as in the trend. A reason for this could be that the differential structure of the absorption cross section for ozone is more distinct in the UV

Huggins Bands than in the visible Chappuis Bands (see figure 3.2 for a plot of the ozone absorption structure).

Because of the better agreement to TOMS and as more continuous data was available from the UV spectrograph only these values were used in the following evaluations. The parameters and the selection of data by NVERT were always kept unchanged.

4.2.2 Long-Term Trend from TOMS Measurements

To put the measurements for 2003 and 2004 into the long-term picture the complete set of EP/TOMS overpass data for Nairobi was plotted in figure 4.3. As comparison the extrapolated (SBUV method) SHADOZ sonde data was given where possible and to indicate the period of focus of this study the 2003/2004 DOAS data set of combined a.m. and p.m. values from the UV fit is shown. The extrapolated sonde data shows a rather good agreement with the satellite data, as was already established in section 3.4. Also the DOAS data seems to agree well with TOMS from this first point of view (see detailed analysis below in section 4.2.3). The EP/TOMS ozone values are always between 220 and 290 DU and show an annual fluctuation, but even more distinct is a biennial cycle which probably can be attributed to the Quasi-Biennial Oscillations (QBO) in the tropics. According to Thompson et al. [2003b] interannual variability of total column ozone above the equator is dominated by the QBO and a complete cycle of these oscillations lies between 1998 and 2000, which agrees with the satellite data. The 2003/2004 time period considered in the following paragraphs also covers exactly one of these biennial (two-year) oscillation periods. Short-term fluctuations of the values are around 20 DU.

Additionally a combined plot of the Nimbus-7 TOMS record from 1979 through 1993 and the Earthprobe TOMS record from 1996 through 2005 is given in figure 4.4. Here the values vary between 220 and 300 DU, while the average is around 260 DU. Annual and biennial oscillations are also clearly distinguishable. To check for long-term trends a line was fitted through the whole data set. This line shows a minimal downwards trend (gradient of -0.077), but actually the Nimbus-7 record shows a slight upwards trend while the Earthprobe values show a slight downwards trend and as the two instruments never operated parallel it is not guaranteed that they are calibrated exactly the same way. Therefore no conclusion of a decline in ozone above Nairobi, the way it is observed in mid and high latitudes, can be drawn. Actually, the record shows a rather good long-term stability.

4.2.3 Comparison of Satellite and Ground-Based Measurements

The main focus of this work lies in the comparison of satellite-born and ground-based measurements in an effort to validate data retrieved from SCIAMACHY. The TOMS data is well verified and can therefore also be used as reference for other measurements.

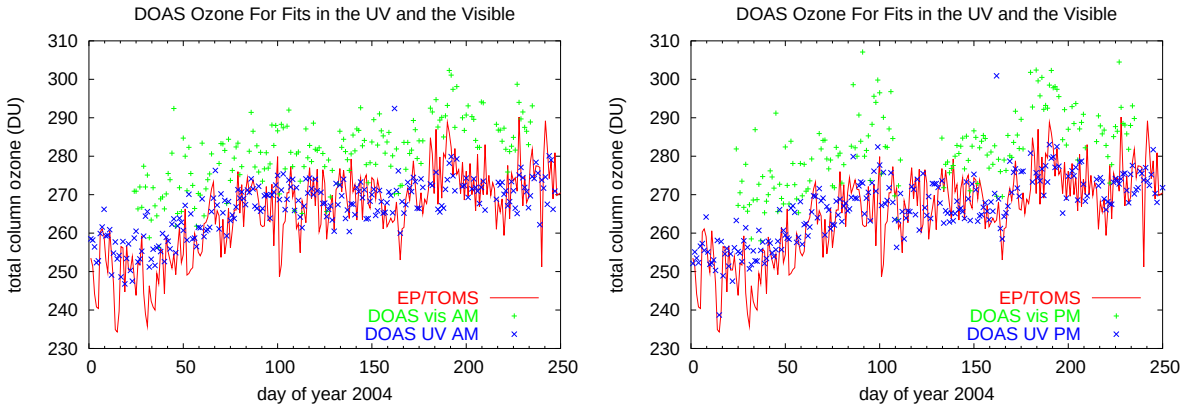

Figure 4.2: *Comparison of DOAS ozone fits in the UV and visible regions. As reference the well verified TOMS measurements are given. The left graph shows a plot for the DOAS a.m. values, the right side for the DOAS p.m. values.*

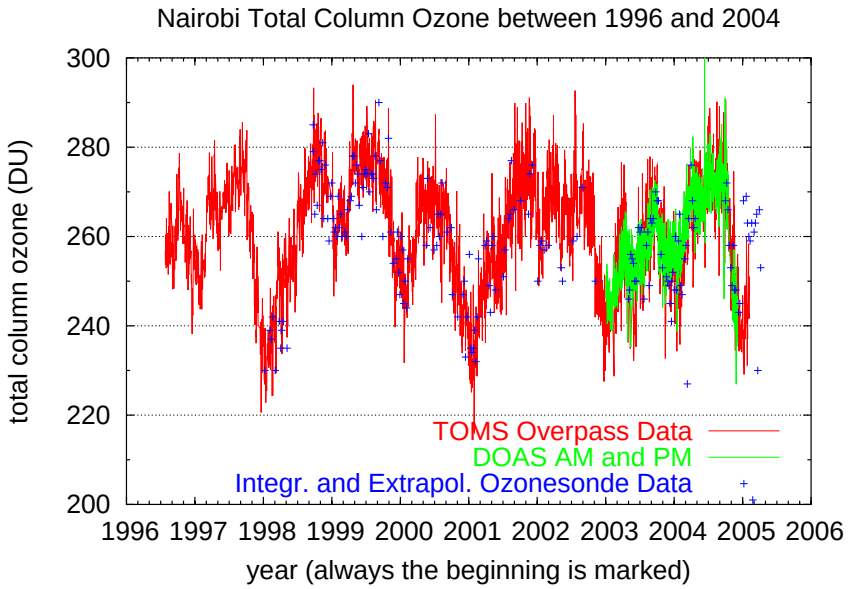

Figure 4.3: *Total column ozone above Nairobi 1996-2005 as recorded by Earthprobe/TOMS. For comparison the DOAS columns for 2003 and 2004 and extrapolated SHADOZ sonde data are given.*

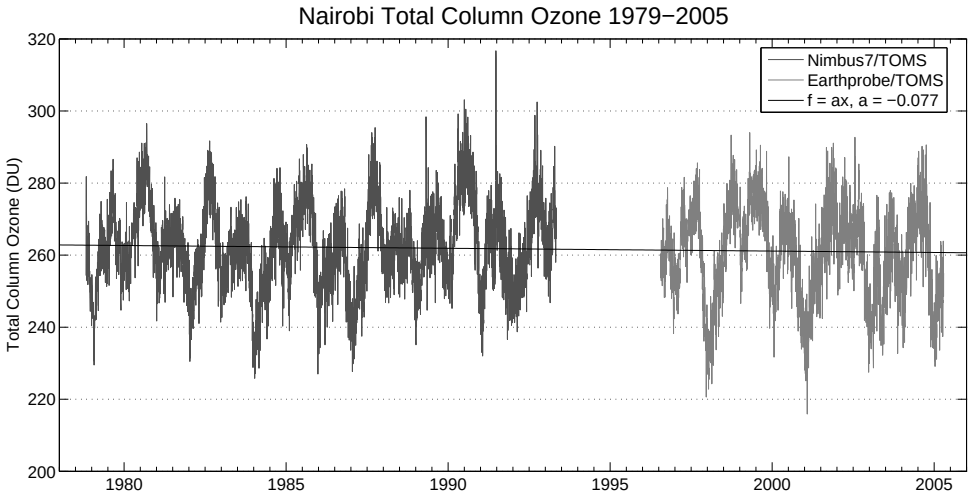

Figure 4.4: *Longterm trend of total ozone above Nairobi as recorded by the TOMS instruments aboard Nimbus-7 and Earthprobe. The straight line is a polynomial fit of first order for the combined data sets.*

The GOME data is by now also well established, but measurements for tropical latitudes were only possible until April 2003. Since then the instrument has only been yielding information for high latitudes. The satellite based DOAS record was continued by the SCIAMACHY instrument, but its measurements are so far less well verified than those of the other satellites.

Records for Nairobi from all these satellite instruments (TOMS, GOME and SCIAMACHY) for the years 2003 and 2004 in comparison with the ground-based DOAS measurements (a.m. values) are given in figure 4.5 together with SHADOZ extrapolated (SBUV method) sonde data. The lower part of the graph shows the percental deviation of the satellite columns from the DOAS columns. In figure 4.6 the same data is plotted, but always for three months at a time.
For a clearer distinction the data from always two instruments are again plotted in figure 4.7, namely DOAS/TOMS, DOAS/SCIAMACHY, TOMS/SCIAMACHY and DOAS/GOME+SHADOZ (as those two records hardly overlap). In these graphs the absolute difference between the records is given.

All the data, except for a few highly unlikely outliers, are in the interval 230 to 290 DU. The mean differences, root-mean-square (RMS) values and maximum differences for same day values between the instruments are given in table 4.3 together with the respective percental values as deviation from DOAS. The extreme outliers of the SCIAMACHY and SHADOZ records (below 235 DU) were ignored. Maximum difference within one day is between TOMS and DOAS records. It is 29.8 DU for DOAS a.m. values and 37.5 for p.m. values. Otherwise, the maximum deviation from DOAS is between 5% and 10% for all instruments.

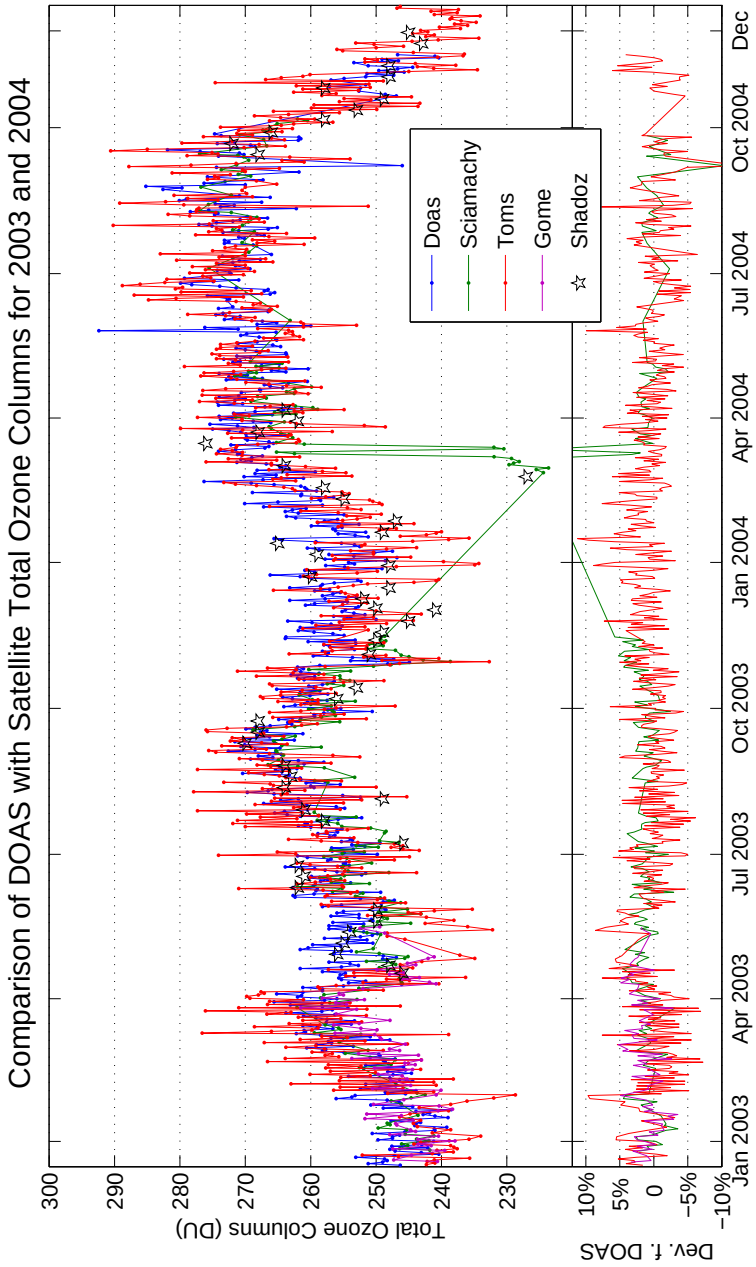

Figure 4.5: *Comparison of DOAS ozone data above Nairobi (a.m. values) for the years 2003 and 2004 with the overpass data of different satellites. The upper part of the graph contains the total column ozone for the different instruments. The lower part of the graph shows the deviation of the satellite values from the DOAS measurements. If available, also extrapolated ozone columns from SHADOZ sonde launches were plotted.*

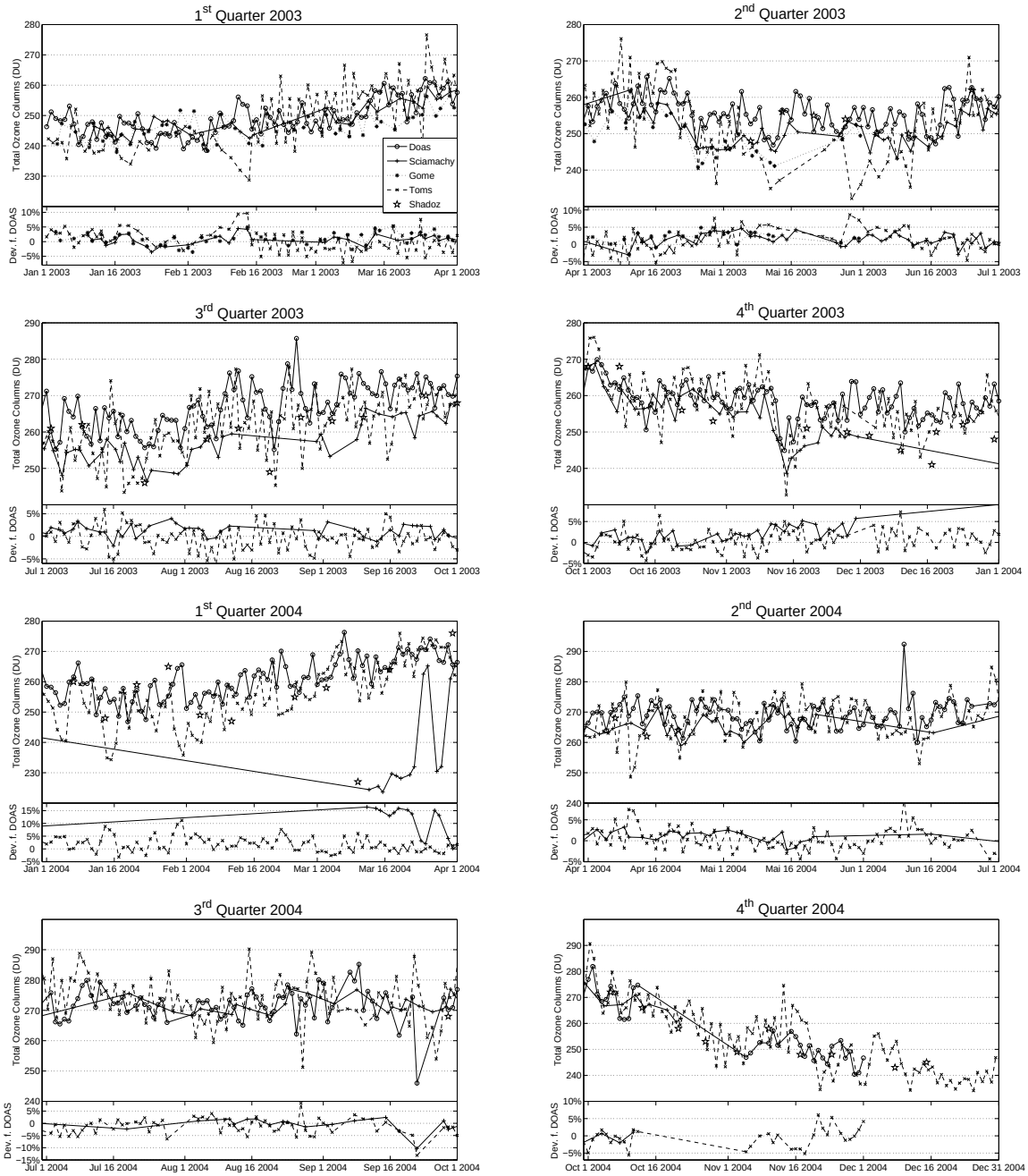

Figure 4.6: *Quarterly comparison of DOAS ozone data above Nairobi (a.m. values) for the years 2003 and 2004 with the overpass data of different satellites. The upper parts of the graphs, each showing a period of three months, contain the total column ozone for the different instruments. The lower parts of the graphs show the deviation of the satellite values from the DOAS measurements. If available, extrapolated ozone columns from SHADOZ sonde launches were plotted as well.*

Table 4.3: *Mean, RMS and maximum values of the differences between the instruments.*

Instruments	Mean	RMS	Max.	Mean %	RMS %	Max. %
DOAS-AM/GOME	3.64	6.2	13.57	1.42%	2.44%	5.24%
DOAS-PM/GOME	2.83	6.36	17.09	1.11%	2.51%	6.62%
DOAS-AM/SCIAMACHY	3.09	5.77	25.35	1.18%	2.23%	10.3%
DOAS-PM/SCIAMACHY	2.08	5.67	20.78	0.78%	2.17%	7.59%
DOAS-AM/TOMS	0.98	8.06	32.2	0.38%	3.1%	13.13%
DOAS-PM/TOMS	-0.17	8.71	37.5	-0.09%	3.37%	14.08%
TOMS/SCIAMACHY	2.08	7.38	19.76	0.71%	2.83%	7.15%
DOAS-AM/SHADOZ	2.4	6.57	18.5	0.92%	2.53%	7.02%
DOAS-PM/SHADOZ	1.18	6.65	14.4	0.42%	2.59%	5.49%
DOAS-AM/DOAS-PM	1.11	5.16	16.3	0.42%	1.98%	6.26%

These statistics confirm the first impression of the graphs that the different data sets agree well. The mean deviations are rather small – being less than 1.5% or 4 DU in absolute values. This indicates a very good agreement in the trend. Also the RMS values of the deviation are never more than 3.5% (less than 9 DU), showing that the difference on single days is slightly higher, but this can be in both directions, as the arithmetic mean value is significantly smaller than the RMS. On average the DOAS measurements are slightly higher than the satellite columns (positive mean difference, except for DOAS-PM/TOMS). Even the maximum deviations are below 10% – only for DOAS/TOMS and DOAS-PM/SCIAMACHY they are between 10% and 15% – and this are only exceptions that can be attributed to outliers, like the two spikes visible in the DOAS plots in June and November 2004. The mean values and RMS of the difference of a satellite instrument and the a.m. and p.m. values of DOAS respectively are never more than 0.5%. This shows that existing deviations are mainly between the different instruments.

A very good agreement of the trends can be concluded from these statistics. There are many factors which can have an influence on the day-to-day measurements resulting in the observed deviations. These possibilities, especially when considering meteorological factors – such as cloud cover (reducing the tropospheric sensibility of satellite instruments and influencing ground-based measurements through additional scattering and reduction of the light intensity), location of the ITCZ and wind fields influencing the transport of trace gases – and the algorithms to retrieve the data, are so plentiful that most of them cannot be discussed at this point. One origin for differences might be that measurements are taken at different times of the day. While the DOAS values are for approximately 7am and 6pm local time, the satellite measurement times are between 10.30am and 12.30am for TOMS, around 10.30am for GOME and around 10am for SCIAMACHY. SHADOZ sondes are usually launched in the morning hours between 7am and 9am. As concluded below (section 4.2.5), the diurnal variation of the total ozone columns is not strong, but the difference between a.m. and p.m. values for DOAS taken with the same instrument already show differences, which leads to the conclusion

that the time factor could be a component of the deviations between the different instruments.
Another factor of influence could be the location of measurement. Ground pixel size for GOME is 40×320 km^2 and for SCIAMACHY it is still 30×60 km^2. The center of the TOMS field of view is usually within 50 km of Nairobi, but can vary to up to 333 km every few days. Ground pixel size for this instrument is 50×50 km^2. Considering only the TOMS data values taken at a distance of more than 100 km from Nairobi (center of field of view) the RMS of the difference rises by only 0.2 DU and when only values of more than 200 km distance are taken it actually drops by 0.5 DU from the value for all available days. The spatial gradient in ozone concentrations should be highest in the troposphere compared to the stratosphere, but the tropospheric ozone is only a minor component in total ozone columns, as outlined below in section 4.2.4. Therefore it is likely that the location factor is not a major influence in the differences between the instruments.

For TOMS and GOME validation efforts have given errors of ±4-5%. This margin is well verified by the RMS values in the comparison of these instruments with DOAS. For SCIAMACHY the RMS values are actually below 3% – also for the comparison with TOMS data – and even the maximum deviations are not higher than for the other instruments. This shows that also this instrument, using the algorithm developed at the IUP Bremen for the analysis, yields very good total column ozone data above Nairobi.

Even if the trend of data from the different instruments agrees very well it is worth taking a closer look at the graphs. TOMS shows the highest short term fluctuation of measured data. Within a few days this can amount to 20 DU, which is also reflected in the slightly higher RMS difference to the DOAS measurements than for the other instruments. For DOAS, GOME and SCIAMACHY these day-to-day fluctuations usually stay in the area of 10 DU. Also for TOMS the data is between 230 and 290 DU, while SCIAMACHY hardly goes out of the interval 240 to 280 DU and DOAS mostly sticks to this region as well.

The TOMS data set is very consistent for the whole time period, showing no gaps in the measurements. It could therefore be said that it is the most reliable instrument. GOME failed for the tropical latitudes after May 2003 and the last month shows a slightly higher difference to the DOAS data, but during May 2003 all the satellite instruments show this deviation from DOAS. The SCIAMACHY data set has a gap between December 2003 and March 2004 and after measurements resumed another month shows highly unlikely data (30-40 DU below the other data sets). The sonde data is far less frequent than all the other instruments, but ignoring the single outlier in March 2004, which could result from an error in the integration or extrapolation calculations, it can be said that this record also agrees very well with the other data sets, especially when considering that it is extrapolated data.

While the correlation between the data sets is good for most of the time with de-

viations roughly centered around zero and hardly reaching over ± 5 %, a slight anti-correlation is visible for some periods. Most prominently is the period between late April and early June 2003, where all the satellite instruments give lower values than DOAS: TOMS and GOME slightly stronger (15-20 DU) than SCIAMACHY (up to 10 DU).
Further periods with an anti-correlation between TOMS and DOAS are January and early February 2003, late November 2003 through March 2004 and another one in June 2004. June 2004 also includes an outlier in the DOAS record which could point to an instrumental factor. The existence of a slight disagreement for the beginning of both years considered could point to a meteorological factor.
For SCIAMACHY disagreement to DOAS is also visible for the third quarter (July-September) of 2003 and again in November 2003 (just before the temporary failure of the SCIAMACHY instrument), while TOMS still agrees better with DOAS.
The more detailed picture of the quarterly graphs shows that also the trends of the short term fluctuations agree rather well, but not completely, for most of the time. This is clearest for a comparison of TOMS and DOAS as for these the available data frequency is highest.

Looking at the long-term development during the whole time period under consideration, the lowest ozone values are seen at the very beginning and in the end with a rather sharp drop in October 2004. Slighter regressions of the total columns are visible during May/June 2003 and between November 2003 and January 2004. No such distinct drop is visible for May/June 2004. Ozone columns for 2004 are generally higher than for 2003 (before the October 2004 drop). During both years values for August/September are slightly higher than during March/April.
Drops in ozone around the change of the year are also visible in the complete EP/TOMS record (see figure 4.3), as outlined above in section 4.2.2. During this longer time period the biennial oscillation is also stronger than the annual one during most years. These annual and biennial variations are likely to stem from meteorological factors, among them the QBO.

4.2.4 Vertical Distribution

To examine the information MAX-DOAS can yield about the vertical distribution of ozone, slant columns for different viewing directions were calculated, while so far only zenith-sky measurements were considered. A wavelength window in the visible was chosen (see table 4.2) for this, where the ozone cross section is less dependant on the temperature and AMFs don't change in large wavelength intervals. Performing a classic fit in the UV region, however, gives a similar result. The result for a sample day in August 2004 is shown in figure 4.8. The good agreement between the different directions indicates an absorber located mostly in the stratosphere, as the longer lightpath through the troposphere in the off-axis directions does not result in an appreciable difference in the columns. Plots for other days of the same year were very similar. This result is not a surprise, but the very good agreement between the different slant columns shows

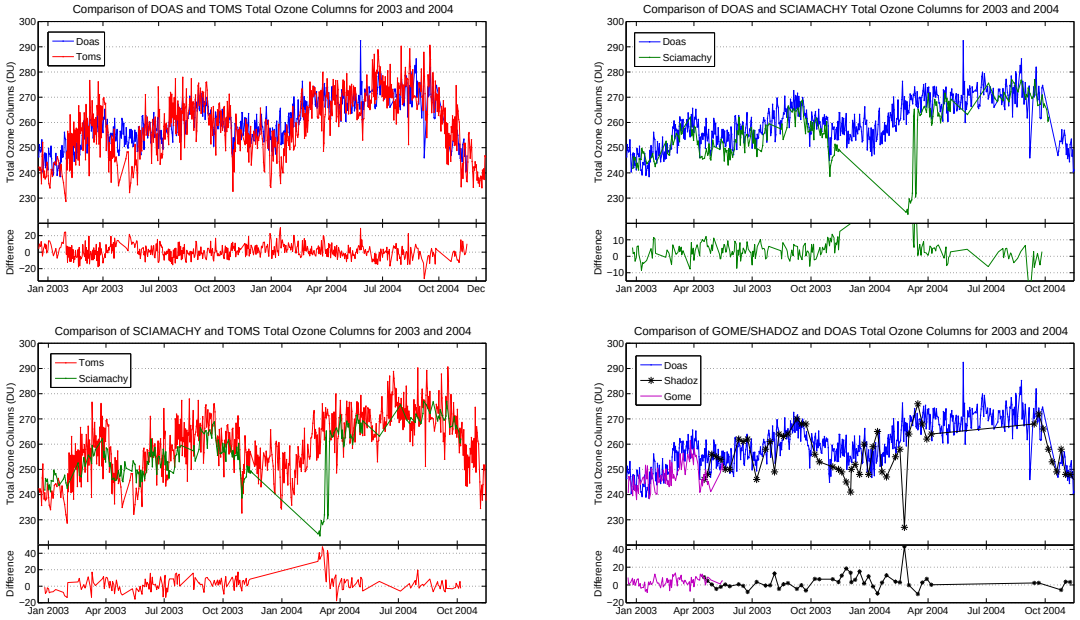

Figure 4.7: *Comparison of the different satellite instruments and SHADOZ sondes with DOAS a.m. values for the years 2003 and 2004.*

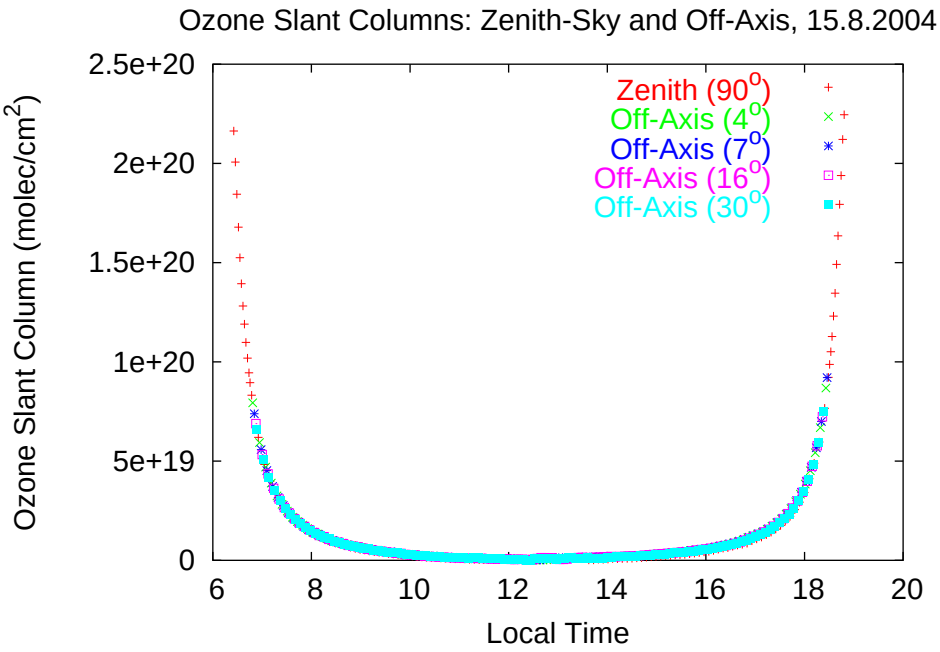

Figure 4.8: *Typical plot of ozone slant columns for different viewing directions for August 15, 2004. The agreement between the different directions clearly indicates a stratospheric absorber.*

that the stratospheric ozone outweighs the tropospheric ozone so much as to make it impossible to obtain any further information about the vertical profile of ozone from the MAX-DOAS measurements.

The vertical distribution is readily available from the sonde measurements. In figure 4.9 all available data for sonde measurements above Nairobi during 2003 and 2004 was plotted to show the temporal development of the vertical ozone profile. White areas in the upper part of the graph are a consequence of preliminary bursts of the balloons. It is clear that most of the ozone resides in the stratospheric ozone layer, with not enough in the troposphere to have an influence on the DOAS off-axis slant columns. Ozone in the planetary boundary level is slightly higher than that in the upper troposphere, but also fluctuates. The concentration in the boundary layer is less during late October through December, which is the time of the short rain season over Nairobi. During the July through October main dry period the values show no drops. For the period of the long rains between late February and June concentration drops in the boundary layer are visible, but not as distinct as during short rains. Near the equator the tropopause has a constant height (in contrast to mid-latitudes) and as expected this comes out in the temporal stability of the vertical distribution with the ozone layer starting at approximately 20 km altitude. After October 2004 a drop in the ozone maximum is observed which is consistent with the drop in total column amounts in figure 4.5 for the same time period.

4.2.5 Diurnal Variation

To evaluate the diurnal variation of ozone above Nairobi the a.m. and p.m. values from the DOAS instrument were taken and illustrated in figure 4.10 together with their difference. The values are the mean of measurements at SZA between 80° and 85° with a fitting error of less than 5%. This means that they are taken approximately at 7am and 6pm (18h) local time. Almost all values stay between 240 and 280 DU. The mean difference between a.m. and p.m. values of the same day for the years 2003 and 2004 is 1.1 DU, the root-mean-square (RMS) value 5.2 DU and the maximum difference for same day values during this period is 16.3 DU. Generally the p.m. values seem to be slightly lower than the a.m. values, but the difference between mean and RMS values shows that this is not very dominant. Also the plot of the difference is pretty well centered around the 0-axis.
During a typical smog situation the afternoon ozone values should be higher than the morning values. Most of the time this is not the case. In July and August higher afternoon values seem to be more common, but the evidence in the plot is not very strong. Variations in stratospheric ozone, where the concentrations are much higher, are more likely to cause these differences in the total columns, but also here evidence does not point to any regular diurnal variation of ozone in the ozone layer.

In figure 4.11 the diurnal variation of vertical columns from the DOAS UV OD-Fit are shown together with the fitting error for two sample days in January and March

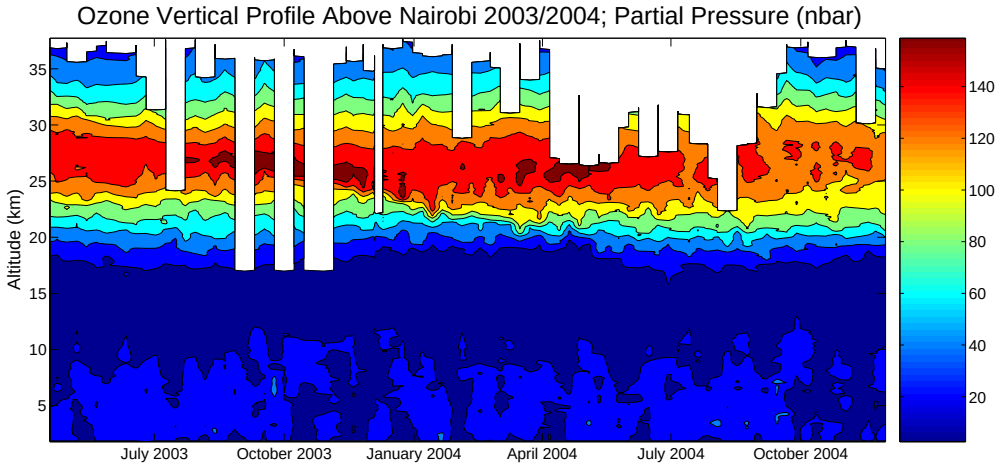

Figure 4.9: *Vertical profile of ozone measured by the SHADOZ ozonesondes above Nairobi for all launches during 2003 and 2004. No data was available for the first 4 months of 2003.*

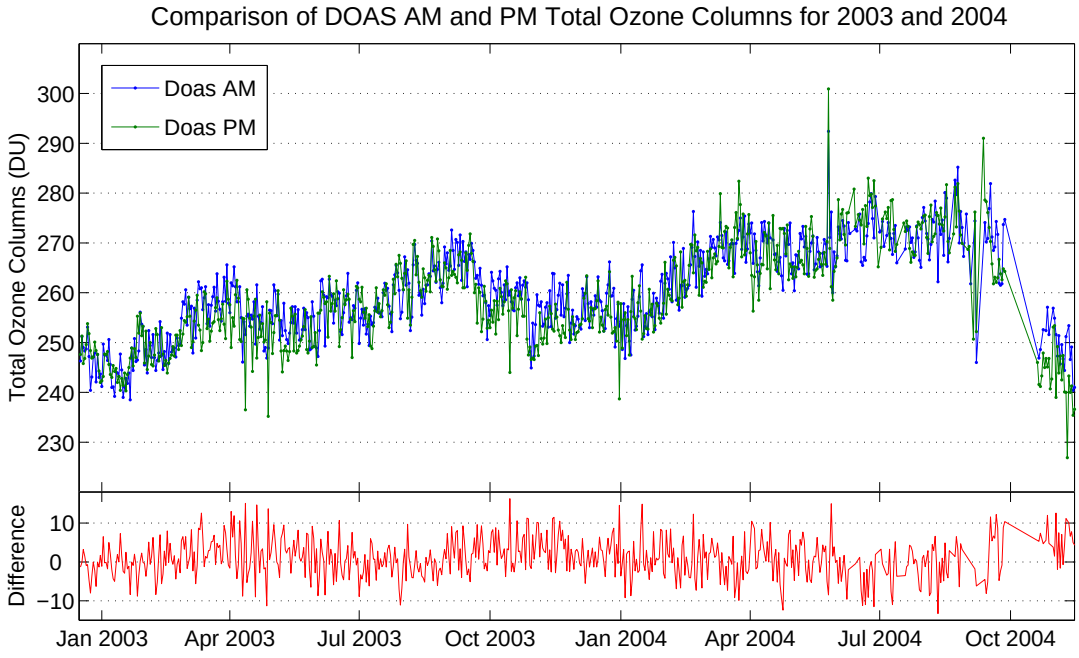

Figure 4.10: *Comparison of Nairobi DOAS columns for a.m. and p.m. hours taken at about 7am and 6pm respectively (80°-85° SZA).*

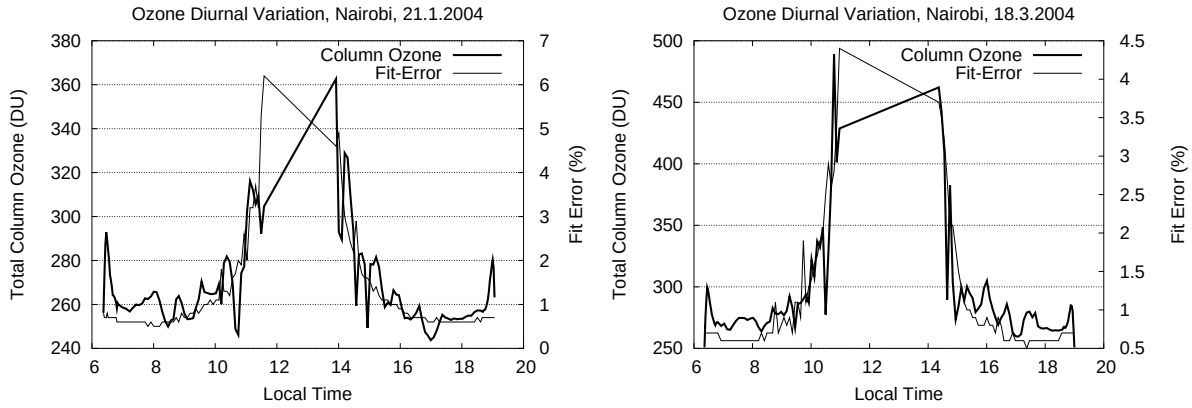

Figure 4.11: *Diurnal variation of ozone vertical columns as measured by the Nairobi DOAS station for two sample days of 2004. The large deviation around noon is a consequence of the use of a noon spectrum for the background during the fit.*

2004. Graphs for other days show very similar developments. The gap in measurements around noon (SZA of less than 20°) is to prevent direct sunlight from entering the telescope, which would severely degrade the data. For the hours before and after this the fitting error is very high and also the ozone columns deviate from those at other times. This is a result of using a same day noon spectrum taken at 21° SZA as background for the fitting process. At SZA close to this the difference between measured and background spectrum is not great enough to get proper results from the DOAS algorithm. Therefore measurements between 10am and 3pm (15h) can not be considered accurate. Additionally small peaks of ozone are seen during the first and last 30 minutes of measurements for both of the days shown. Also these do not seem to be the result of an actual variation in the ozone columns, but an effect of the measurement process. The AMF might not properly account for SZA greater 90° where the sun is still below the horizon.

Actually, this effect in zenith sky ozone observations of first rising and then falling slant columns around sunrise and sunset has been used since the 1930s in the so called "Umkehr Method" developed by Götz to estimate the altitude of the ozone layer [Dobson, 1968]. This effect is due to the fact that at very low SZA most light reaching the zenith sky telescope is scattered above the ozone layer. With decreasing SZA the most probable scattering height goes down and once it lies within the ozone layer the ozone column appears to be greater. With the SZA and so the scattering altitude decreasing further the measured ozone values go down again. It might be that this effect is not properly accounted for in the AMF for great SZA thus resulting in the observed peaks in the retrieved vertical columns.

Otherwise, the values show a fluctuation of around 10-15 DU within the day. For January 21 the afternoon values are clearly lower than morning values, while they seem rather constant on March 18. It is a possibility that meteorological factors account for this fluctuation. The trends are, however, too unclear to allow for any more conclusive interpretation.

5 Summary and Conclusion

In this work satellite ozone data from the TOMS, GOME and SCIAMACHY instruments was compared to total column ozone retrieved with the ground-based DOAS station in Nairobi using a fit in the UV region for the years 2003 and 2004.

It was first established, that for ozone DOAS fitting in the UV region yields better results than if done in the visible. This could be due to the more distinct absorption cross section in the UV Huggins Bands compared with the Chappuis Bands (visible).

The long-term trend of TOMS, the instrument that has given the longest record available, was shown; annual and biennial (two-year) oscillations between 40 and 60 DU are clearly visible, while the average lies at 260 DU. A good long-term stability was detected, implying no depletion of the total ozone columns.

From the mean and RMS values of the difference between the DOAS, TOMS, GOME and SCIAMACHY instruments and the sonde data it was concluded that they show a very good agreement in trend. The mean differences are never above 4 DU, which is a deviation of less than 1.5%, and the RMS values don't go above 9 DU or 3.5%. Especially the lower mean differences show that the trend agrees well, while there are slightly higher short term deviations. Part of this difference could be a result of the measurements not being carried out simultaneously. However, the existing variation in measurement location for the satellite instruments does not seem to have much influence in the tropical region, as was shown from the RMS values of TOMS for changing distance of the measurements. On the other hand, there are so many meteorological factors influencing the results and the algorithms to calculate them are so complex that the observed deviations cannot be clearly assigned to any of these. The observed RMS values agree well with margins set by other validation efforts for TOMS and GOME.

TOMS shows a slightly higher short term fluctuation than the other instruments: 20 instead of 10 DU. The interval in which the data is scattered is slightly bigger as well, being between 230 and 290 DU, instead of between 240 and 280 DU. On the other hand, TOMS is the most reliable of the instruments in terms of the temporal coverage. It gives daily measurements and has hardly ever failed in comparison to all other systems. The least reliability in this sense is that of the SHADOZ ozonesondes, but nonetheless they are not the best method to retrieve total column ozone and their extrapolated data was only included for comparison.

Correlation between the different data sets is very good during most of the time considered: The deviation is centered roughly around zero and hardly goes beyond $\pm$ 5%. During late April and early June 2003 most instruments disagree with DOAS – this is the most distinct feature. TOMS also disagrees with DOAS around the turning of the

years. SCIAMACHY shows a few periods of slight disagreement with DOAS during 2003, especially during the third quarter of the year.

The long-term picture shows regressions around the turns of the years, more distinctly for the beginning of 2003 and the end of 2004 than at the turn of these years. This, in agreement with the longer TOMS record, shows a clear annual and biennial variation. The latter implies that exactly one cycle of the Quasi-Biennial Oscillations is covered in this report. Further studies linking these variations with the influence of the QBO of global wind fields have been done [Thompson et al., 2003b, and references therein].

Focusing on the validation of SCIAMACHY the evidence from the considered comparisons show that for the Nairobi location the Bremian algorithm yields good results for the total ozone data received from this instrument's measurements. ENVISAT does not pass over every equatorial location on a daily basis and so the data record is less frequent. A failure during December 2003 through March 2004 suggests less reliability for continuous measurements than for example given by TOMS, an instrument with a much simpler setup. There are some slight anti-correlations to the other instruments, but generally SCIAMACHY shows very good agreement to DOAS and TOMS and represents the trends very well – the mean and RMS values of the deviation from DOAS actually being a little better than for the other records. SCIAMACHY also shows less short term fluctuation than TOMS. In conclusion this instrument will definitely make valuable contributions to atmospheric science, especially as total columns of ozone are only one of its many features.

An analysis of the vertical distribution of ozone using sonde data and the DOAS off-axis measurements shows that stratospheric ozone outweighs tropospheric amounts so far that a separation of these atmospheric layers seems very hard for the remote sensing instruments considered. For the DOAS instrument in Nairobi the ozone slant columns of different viewing directions are so close to each other that no separation of the tropospheric information (for example about the Nairobi smog situation) can be expected to be possible. This is different for other absorbers with a not so strong stratospheric dominance, like NO_2 [Adupko, 2002]. Efforts are being undertaken to achieve a troposphere/stratosphere separation for the different satellite instruments, for example for TOMS [Martin et al., 2002]. Similar ambitions exist for SCIAMACHY and should be followed up, especially with the potential to do so for many different trace gases.

An examination of the diurnal variation observed by DOAS suggests a relative stability of the total ozone columns. Most of the existing stronger fluctuations can be attributed to instrumental effects: A longer period around noon does not yield reliable information due to the impossibility of zenith-sky measurements at very small SZA and the use of a noon background spectrum, which makes calculations for SZA close to the one of the background spectrum highly unreliable. For sunrise and sunset a rise in ozone is observed that could be a result of the "Umkehr Effect" not being completely

considered in the OD-Spectrum for great SZA. Smaller fluctuations might be a result of weather changes, e.g. cloud cover.

As this study has shown very good agreement between the different ozone data sets for Nairobi, further work could examine the trend agreement of SCIAMACHY and DOAS for other absorbers.

While information on tropospheric ozone can not be obtained from DOAS in Nairobi, this looks more promising for other trace gases, which would be worth further investigation. A retrieval for tropospheric columns from the measurements in the off-axis directions has been recently written at the IUP Bremen and gives promising results for NO_2. The regional wind fields, however, make it unlikely to retrieve a signal from the African biomass burning regions [S. Fietkau, private communication]. Further work to examine traffic pollution, but maybe even waste burning and other city emissions, would now be desirable.
For ozone measurements related to the smog situation in Nairobi chemical in-situ monitoring at representative sites (traffic artery, industrial, less polluted), comparable to air quality monitoring networks in German cities, would be more practical. Another possibility lies in LIDAR observations, which have a very good spatial resolution, but are costly.

For the continuous verification of satellite measurements and to obtain records of long-term observations it is very desirable to keep up the Nairobi DOAS station. Dobson spectrometers have yielded a very valuable record of total column ozone in many places around the world, but the clear advantage of DOAS is the different absorbers it can observe. As tropical data is still scarce and many more stations are operated in mid and high latitudes a special focus should be laid on maintaining the observations in Nairobi. The launch of SHADOZ ozonesondes nearby provides another valuable addition. Therefore every effort should be made not only to operate the instrument, but also to continuously evaluate the retrieved data.

Abbreviations

AMF	Air Mass Factor
BREDOM	Bremian DOAS Network for Atmospheric Measurements
CCD	Charge Coupled Device (Detector)
CMR	Constant Mixing Ratio
DMSP	Defense Meteorological Satellite Program
DOAS	Differential Optical Absorption Spectroscopy
DSCD	Differential Slant Column Density
DU	Dobson Units
ENSO	El-Niño/Southern Oscillations
EOS	Earth Observation System
EP/TOMS	Earthprobe Total Ozone Mapping Spectrometer
ERS-2	Second European Remote Sensing Satellite
ESA	European Space Agency
GOME	Global Ozone Monitoring Experiment
GSFC	Goddard Space Flight Center
ITCZ	InterTropical Convergence Zone
IUP	Institut für UmweltPhysik (Institute of Environmental Physics)
MAX-DOAS	Multi-AXis DOAS
MPI	Max Planck Institut für Chemie, Mainz
NASA	National Aeronautics and Space Administration
NIR	Near InfraRed
OD	Optical Depth
OMI	Ozone Monitoring Instrument
QBO	Quasi-Biennial Oscillations
RMS	Root-Mean-Square Value
RTM	Radiative Transfer Model
SBUV	Solar Backscattered Ultraviolet Spectrometer
SC	Slant Column
SCIAMACHY	SCanning Imaging Absorption spectroMeter for Atmospheric CHartographY
SHADOZ	Southern Hemisphere Additional Ozonesondes
STE	Stratospheric-Tropospheric Exchange
SZA	Solar Zenith Angle
TOMS	Total Ozone Mapping Spectrometer
UNEP	United Nations Environmental Program, based in Nairobi
UoN	University of Nairobi
UV	Ultra-Violet (light)
VC	Vertical Column
VOCs	Volatile Organic Compounds
VOD	Vertical Optical Depth
WMO	World Meteorological Organisation

List of Figures

List of Tables

References

Adupko, D.C. (2002), Characterisation of a MAX-DOAS Instrument and Application to Satellite Validation, Master Thesis, University of Bremen. (`www.iup.physik.uni-bremen.de/doas/paper/adukpo_thesis.pdf`)

Akeem, A.O. (2003), The FUll Retrieval Method [FURM] Analysis of the Effects of Biomass Burning Emissions on Tropical Tropospheric Ozone, Master Thesis, University of Bremen. (`www.iup.physik.uni-bremen.de/doas/paper/mastersthesis_amaoakeem_sep2003.pdf`)

Borrell, P., J.P. Burrows, U. Platt, A. Richter and T. Wagner (2003), New Directions: New Developments in Satellite Capabilities for Probing the Chemistry of the Troposphere, *Atmospheric Environment*, **37**, 2567-2570. (`www.iup.physik.uni-bremen.de/doas/paper/ae_03_borrell.pdf`)

Bovensmann, H., J.P. Burrows, M. Buchwitz, J. Frerick, S. Noël, V.V. Rozanov, K.V. Chance, and A.H.P. Goede (1999), SCIAMACHY – Mission objectives and measurement modes, *J. Atmos. Sci.*, **56(2)**, 127-150.

Brimblecombe (1996), Air Composition & Chemistry, Cambridge University Press.

Burrows, J.P., M. Weber, M. Buchwitz, V. Rozanov, A. Ladstätter-Weißenmayer, A. Richter, R. DeBeek, R. Hoogen, K. Bramstedt, K.-U. Eichmann, M. Eisinger und D. Perner (1999a), The Global Ozone Monitoring Experiment (GOME): Mission Concept and First Scientific Results, *J. Atmos. Sci*, **56**, 151-175.

Burrows, J.P., M. Buchwitz, M. Eisinger, V. Rozanov, M. Weber, A. Richter and A. Ladstätter-Weißenmayer (1999b), The Global Ozone Monitoring Experiment (GOME): Mission, Instrument Concept, and First Scientific Results, *ESA, 3rd ERS symposium*. (`earth.esa.int/workshops/ers97/papers/burrows1/`)

Chapman, S. (1930), A theory of upper-atmospheric ozone, *Mem. Roy. Meteorol. Soc.*, **3**, 103.

de Beek, R., M. Vountas, V. Rozanov, A. Richter and J.P. Burrows (2001), The Ring Effect in the cloudy atmosphere, *Geophysical Research Letters*, **28(4)**, 721-724. (`www.iup.physik.uni-bremen.de/doas/paper/grl_01_debeek.pdf`)

Dobson, G.M.B. (1968), Forty Years' Research on Atmospheric Ozone at Oxford: a History, *Applied Optics*, **7(3)**, 387-405.

EarthProbe TOMS (Total Ozone Mapping Spectrometer) V.8 Overpass Data above Nairobi (1.27 °S, 36.8 °E), NASA Goddard Space Flight Center. (`ftp://jwocky.gsfc.nasa.gov/pub/eptoms/data/overpass/OVP175_ept.txt`)

Edwards, D.P., J.-F. Lamarque, J.-L. Attié, L.K. Emmons, A. Richter, J.-P.Cammas, J.C. Gille, G.L. Francis, M.N. Deeter, J. Warner, D.C. Ziskin, L.V. Lyjak, J.R. Drummond and

J.P. Burrows (2003), Tropospheric ozone over the tropical Atlantic: A satellite perspective, *Journal of Geophysical Research*, **108(d8)**. (`www.iup.physik.uni-bremen.de/doas/paper/jgr_03_edwards_o3.pdf`)

Eskes, H.J. and K.F. Boersma (2003), Averaging kernels for DOAS total-column satellite retrievals, *Atmos. Chem. Phys.*, **3**, 1285-1291. (`www.atmos-chem-phys.org/acp/3/1285/`)

Hanel, R.A., B.J. Conrath, D.E. Jennings and R.E. Samuelson (2003), Exploration of the Solar System by Infrared Remote Sensing, Cambridge University Press.

Hobbs, P.V. (2000), Introduction to Atmospheric Chemistry, Cambridge University Press.

Hönninger, G, C. von Friedeburg and U. Platt (2004), Multi axis differential optical absorption spectroscopy (MAX-DOAS), *Atmos. Chem. Phys.*, **4**, 231-254. (`www.atmos-chem-phys.org/acp/4/231/`)

IPCC (2001), Climate Change 2001: The Scientific Basis. Contribution of Working Group I to the Third Assessment Report of the Intergovernmental Panel on Climate Change [Houghton, J.T.,Y. Ding, D.J. Griggs, M. Noguer, P.J. van der Linden, X. Dai, K. Maskell, and C.A. Johnson (eds.)]. Cambridge University Press, Cambridge, United Kingdom and New York, NY, USA, 881pp.

Kunhikrishnan, T., M.G. Lawrence, R. von Kuhlmann, A. Ladstätter-Weißenmeier and J.P. Burrows (2004), Semiannual NO2 plumes during the monsoon transition periods over the central Indian Ocean, *Geophysical Research Letters*, **31**. (`www.iup.physik.uni-bremen.de/doas/paper/grl_04_kunhikrishnan.pdf`)

Ladstätter-Weißenmeier, A., J. Meyer-Arnek, A. Schlemm and J.P. Burrows (2004), Influence of stratospheric airmasses on tropospheric vertical O_3 columns based on GOME (Global Ozone Monitoring Experiment) measurements and backtrajectory calculation over the Pacific, *Atmos. Chem. Phys.*, **4**, 903-909. (`www.atmos-chem-phys.org/acp/4/903/`)

Martin, R.V., et al. (2002), Interpretation of TOMS observations of tropical tropospheric ozone with a global model and in situ observations, *J. Geophys. Res.*, **107(D18)**, 4351.

McPeters, R.D., P.K. Bhartia, A.J. Krueger, J.R. Herman, C.G. Wellemeyer, C.J. Seftor, G. Jaross, O. Torres, L. Moy, G. Labow, W. Byerly, S.L. Taylor, T. Swissler and R.P. Cebula (1998), Earth Probe Total Ozone Mapping Spectrometer (TOMS) Data Products User's Guide, *NASA Technichal Publication*, 1998-206895.

Nimbus7 TOMS (Total Ozone Mapping Spectrometer) V.8 Overpass Data, NASA Goddard Space Flight Center. (`ftp://jwocky.gsfc.nasa.gov/pub/nimbus7/data/overpass/`)

Oreskes, N. (2004), Beyond the Ivory Tower: The Scientific Consensus on Climate Change, *Science*, **306**. (`www.sciencemag.org/cgi/content/full/306/5702/1686`)

Noxon, J.F., E.C. Whipple Jr., and R.S. Hyde (1979), Stratospheric NO_2 1. Operational method and behaviour at mid-latitude, *J. Geophys. Res.*, **84**, 5047-5065.

Perner, D. and U. Platt (1979), Detection of Nitrous Acid in the atmosphere by differential absorption, *Geophys. Res. Lett.*, **6**, 917-920.

Richter, A., M. Eisinger, A. Ladstätter-Weißenmeier and J.P. Burrows (1999a), Sky Observations: 2. Seasonal Variation of BrO over Bremen (53°N) 1994-1995, *Journal of Atmospheric Chemistry*, **32**, 83-99. (`www.iup.physik.uni-bremen.de/doas/paper/JAC_99_richter.pdf`)

Richter, A., H. Kreher, P.V. Johnston, F. Wittrock and J.P. Burrows (1999b), Validation of GOME O_3, NO_2, BrO and OClO Measurements in Southern High Latitudes, *Fifth European Workshop on Stratospheric Ozone, St. Jean de Luz, France*. (`www.iup.physik.uni-bremen.de/doas/paper/sjdl_99_richter2.zip`)

Richter, A. (1997), Absorptionsspektroskopische Messungen Stratosphärischer Spurengase Über Bremen, 53°N, PhD Thesis (Dissertation), University of Bremen. (`www.iup.physik.uni-bremen.de/doas/paper/diss_97_richter.zip`), (German)

Rozanov, A., V. Rozanov, and J.P. Burrows (2001), A numerical radiative transfer model for a spherical planetary atmosphere: Combined differential-integral approach involving the Picard iterative approximation, *Journal of Quantitative Spectroscopy and Radiative Transfer*, **69**, 4135-4142.

Rozanov, V., D. Diebel, R. Spurr, and J.P. Burrows (1997), GOMETRAN: A radiative transfer model for the satellite project GOME – the plane parallel version, *J. Geophys. Res.*, **102**, 16683-16695.

Sanders, R.W., S. Solomon, J.P. Smith, L. Perliski, H.L. Millr, G.H. Mount, J.G. Keys, and A.L. Schmeltekopf (1993): Visible and Near-Ultraviolet Spectroscopy at McMurdo Station Antarctica, 9. Observations of OCIO from April to October 1991, *J. Geophys. Res.*, **98(D4)**, 7219-7228.

SHADOZ (Southern Hemisphere Additional Ozonesondes) Data, WMO/GAW Global Station Nairobi (1.27 °S, 36.8 °E). (`croc.gsfc.nasa.gov/shadoz/Nairobi.html`)

Stutz, J., and U. Platt (1996), Numerical Analysis and Estimation of the Statistical Error of Differential Optical Absorption Spectroscopy Measurements with Least-Squares methods, *Applied Optics*, **35(30)**, 6041-6053.

Thiongo, K. (1998), Characteristics of vertical profile Ozone near the equator, Nairobi University Press.

Thompson, A., J. Witte, S. Oltmans and F. Schmidlin (2004), SHADOZ – A Tropical Ozonesonde-Radiosonde Network for the Atmospheric Community, *Bulletin of the American Meteorological Society*, **Oct**. (`ams.allenpress.com/pdfserv/10.1175/BAMS-85-10-1549`)

Thompson, A.M., J.C. Witte, R.D. McPeters, S.J. Oltmans, F.J. Schmidlin, J.A. Logan, M. Fujiwara, V.W.J.H. Kirchhoff, F. Posny, G.J.R. Coetzee, B. Hoegger, S. Kawakami, T. Ogawa, B.J. Johnson, H. Vömel and G. Labow (2003a), Southern Hemisphere Additional Ozonesondes (SHADOZ) 1998-2000 tropical ozone climatology 1. Comparison with Total Ozone Mapping Spectrometer (TOMS) and ground-based measurements, *J. Geophys. Res.*, **108(D2)**, 8238.

Thompson, A.M., J.C. Witte, S.J. Oltmans, F.J. Schmidlin, J.A. Logan, M. Fujiwara, V.W.J.H. Kirchhoff, F. Posny, G.J.R. Coetzee, B. Hoegger, S. Kawakami, T. Ogawa, J.P.F. Fortuin and H.M. Kelder (2003b), Southern Hemisphere Additional Ozonesondes (SHADOZ) 1998-2000 tropical ozone climatology 2. Tropospheric variability and the zonal wave-one, *J. Geophys. Res.*, **108(D2)**, 8241.

Thompson, A., J. Witte, R. Hudson, H. Guo, J. Herman and M. Fujiwara (2001), Tropical Tropospheric Ozone and Biomass Burning, *Science*, **291**, 2128-2132.

Warneck, P. (1988), Chemistry of the Natural Atmosphere, International Geophysics Series Volume 41, Academic Press.

Wittrock, F., H. Oetjen, A. Richter, S. Fietkau, T. Medeke, A. Rozanov, and J.P. Burrows (2004), MAX-DOAS measurements of atmospheric trace gases in Ny-Ålesund – Radiative transfer studies and their application, *Atmos. Chem. Phys.*, **4**, 955-966. (`www.atmos-chem-phys.org/acp/4/955/`)

Acknowledgement

First of all I would like to thank everyone who made this project possible. Foremost Dr. Angeyo Kalambuka at the University of Nairobi and Sixten Fietkau at the University of Bremen, both having done a great job supervising and supporting me in my work. Additional thanks goes to Joannes Berque, Dr. Kaduki (UoN) and Prof. Burrows (Bremen), who all helped make this project possible.
I would also like to acknowledge NASA's Goddard Space Flight Center for providing SHADOZ and TOMS data through their website, as well as the DOAS group at the University of Bremen's Institute of Environmental Physics for the MAX-DOAS data and the processed GOME and SCIAMACHY data.

My special thanks goes to Dr. Jürgen Theiss, who invests a lot of time and energy in the coordination of the Berlin-Nairobi-Exchange, and everyone else involved in this exchange for making it possible for me to stay one year studying in Kenya. I would also like to thank Prof. Aduda and all the staff at the Physics Department and the University of Nairobi for accepting and welcoming me as an exchange student for the academic year 2004/2005.

Sebastian and Christopher, you were great friends sharing the time and experience in Nairobi. Many greetings to all the students at UoN who were so friendly to us during this year.

Thanks to my parents, my grandparents and my brother who have always been supportive, not only when I decided to go to Nairobi.